ACCSCIENCE PUBLISHING
An International Journal of Optimization and Control: Theories & Applications
ISSN: 2146-0957 eISSN: 2146-5703
Vol.16, No.3, pp.1179-1215 (2026)
https://doi.org/10.36922/IJOCTA026090034
IJOCTA
RESEARCH ARTICLE

External-field optimality of logarithmic coeffcients with applications to geometric image analysis

Rabha W. Ibrahim[1,2†*], Dumitru Baleanu[3†], and Soheil Salahshour[4,5]

[1]Department of Mathematics, Saveetha School of Engineering , Saveetha Institute of Medical and Technical Sciences SIMATS, Chennai, Tamil Nadu, India
[2]Information and Communication Technology Research Group, Scientific Research Center, Al-Ayen University, Thi-Qar, Nasiriyah, Iraq
[3]Department of Computer Science and Mathematics, Lebanese American University, Beirut, Lebanon
[4]Advanced Computing Lab, Faculty of Engineering and Natural Sciences, Istanbul Okan University, Turkey
[5]Faculty of Engineering and Natural Sciences, Bahcesehir University, Istanbul, Turkey
rabhaibrahim133@gmail.com, dumitru.baleanu@gmail.com, soheil.salahshour@okan.edu.tr

ARTICLE INFO

Article History:
Received: March 1, 2026
Revised: March 23, 2026
Accepted: March 26, 2026
Published Online: June 9, 2026

Keywords:
Logarithmic coefficients;
Analytic function
Herglotz representation
Coefficient bounds
Univalent function
Image processing
Open unit disk
Extremal problems
Optimal bound
Multiplier-defined subclasses

AMS Classification 2010:
26A33; 34A08; 35H15;
34K50 47H10; 60H10

ABSTRACT

This paper develops an external-field optimization framework for logarithmic coefficients of multiplier-defined univalent functions and establishes optimality principles with applications to geometric image analysis. Using the Herglotz representation, logarithmic coefficients are expressed as nonlinear moment functionals of probability measures on the unit circle, where multiplier coefficients act as an external field imposing admissibility constraints. A general Euler–Lagrange condition is derived, yielding a nonlinear equilibrium equation that characterizes extremal solutions. When the external-field potential admits a unique maximizer, the extremal measure collapses to a one-point distribution, leading to explicit optimal special-function solutions. The theoretical framework is applied to a dataset of citrus lesion images. After segmentation and conformal normalization of lesion regions, approximate logarithmic coefficients are computed from boundary harmonic expansions. A distortion index and harmonic separation criterion are introduced, and a coefficient separation theorem is verified numerically, demonstrating that geometric differences in lesion morphology correspond to measurable differences in logarithmic coefficient distributions. The results provide a mathematically rigorous connection between nonlinear external-field optimization, conformal special-function representations, and shape-based image descriptors. This approach offers a theoretically grounded and conformally invariant methodology for analyzing geometric irregularity in biomedical and agricultural imaging.

1. Introduction

The study of logarithmic coefficients of univalent functions has been a central topic in geometric function theory since the early works of Lebedev, de Branges, and others (for recent efforts [1–3]). Given a normalized univalent function $f(z) = z + \sum_{n=2}^{\infty} a_n z^n$ in the unit disk $\mathbb{D}$ denoting by $\mathcal{S}$, the logarithmic coefficients $\{\gamma_n\}$ defined by

$$\log \frac{f(z)}{z} = 2 \sum_{n=1}^{\infty} \gamma_n z^n \qquad (1)$$

encode subtle geometric information about f and play a critical role in distortion theorems, coefficient problems, and inequalities connected to conformal mapping [4–6]. While the second and third logarithmic coefficients have been widely studied and sharp estimates are known in numerous function classes [7–9], the determination of higher-order coefficients remains a challenging open problem in geometric function theory ([10–12]). One powerful approach to this problem is the introduction of *multiplier-defined*

*Corresponding Author
†*These authors contributed equally to this work.*

classes, where a polynomial $M(z) = 1 + \mu_1 z + \mu_2 z^2 + \cdots + \mu_d z^d$ acts as a weight, and the defining condition $\Re\{M(z)f'(z)\} > 0$ ensures univalence together with analytic control over the coefficients. Special cases, such as $M(z) = 1 - z$, $M(z) = 1 - z^2$, $M(z) = (1 - z)^2$, and $M(z) = 1 - z + z^2$, generate classical subclasses of close-to-convex, starlike, and related families of univalent functions. These classes have been studied extensively because they interpolate between convexity and starlikeness while allowing sharper control of coefficient bounds [13].

Recent contributions have highlighted the importance of logarithmic coefficients in connection with extremal problems, and growth-distortion estimates. However, most existing results are restricted to low orders $(\gamma_2, \gamma_3, \gamma_4)$, and there is a clear need for a general framework capable of producing sharp or near-sharp bounds for arbitrary γ_n. Such bounds are particularly valuable because they give insight into the global behavior of analytic maps and provide test cases for conjectures in conformal geometry.

Geometric image analysis focuses on extracting shape-based descriptors from segmented regions rather than relying on pixel-level texture or statistical intensity features. In the present framework, each lesion region is modeled as a simply connected planar domain $\Omega \subset \mathbb{C}$, obtained via segmentation and boundary extraction. Through conformal normalization $f : \mathbb{D} \to \Omega$ with $f(0) = 0$ and $f'(0) = 1$, the lesion boundary geometry is encoded in the logarithmic coefficients Equation (1). These coefficients represent harmonic boundary deformation modes, where lower-order terms capture global anisotropy and higher-order terms quantify boundary roughness and oscillatory irregularity. The resulting distortion index, as shown in Equation (2)

$$\mathcal{D}(r) = 2\sum_{k\geq 1} |\gamma_k| r^k \tag{2}$$

provides a conformally invariant measure of geometric complexity. Thus, lesion morphology is translated into a structured harmonic feature representation, enabling mathematically interpretable shape comparison across image datasets. The main contributions of this work are summarized as follows. First, we reformulate logarithmic coefficient problems for multiplier-defined univalent functions as constrained nonlinear optimization problems over Herglotz measures, where the multiplier coefficients act as an external field. Second, a general external-field Euler-Lagrange principle is established, yielding a nonlinear equilibrium equation that characterizes extremal configurations explicitly. Third, sharp upper bounds for higher-order logarithmic coefficients are derived within this variational framework, unifying and extending several classical multiplier subclasses. Fourth, it is shown that when the external-field potential admits a unique maximizer, the extremal measure collapses to a one–point distribution, leading to closed–form solutions expressed through logarithmic and exponential special functions. Finally, this external-field perspective provides a systematic analytical mechanism for solving nonlinear optimization problems and nonlinear equations with weighted or fractional–type constraints, thereby bridging geometric function theory, nonlinear optimization, and special-function methods.

2. Generalized multiplier formulation

In geometric function theory, multiplier operators are frequently introduced through low-degree generating functions in order to control the contribution of the first few harmonic deformation modes of the boundary. A particularly important case is the quadratic multiplier, as defined in Equation (3):

$$M(z) = 1 + \mu_1 z + \mu_2 z^2 \tag{3}$$

where $\mu_1, \mu_2 \in \mathbb{R}$ are parameters. Such multipliers modify the logarithmic expansion Equation (1) by assigning weights to the first two harmonic modes, which correspond to anisotropic deformation and higher-order boundary curvature effects. Quadratic multipliers therefore provide a convenient mechanism for controlling the second- and third-order coefficient behavior of analytic functions.

To place to place our results in a broader analytic and potential-theoretic context, we introduce a generalized multiplier of arbitrary degree (Equation (4)):

$$M(z) = 1+\mu_1 z+\mu_2 z^2+\cdots+\mu_n z^n,\ \mu_j \in \mathbb{R},\ n \geq 1 \tag{4}$$

We consider the class $\mathcal{F}(M)$ of analytic functions $f \in \mathcal{S}$ with $f''(0) > 0$, satisfying Equation (5):

$$\Re\{M(z)f'(z)\} > 0, \qquad z \in \mathbb{D} \tag{5}$$

The Carathéodory reduction and Herglotz representation can be defined as Equation (6):

$$p(z) := M(z)f'(z) \tag{6}$$

Then p belongs to the Carathéodory class $\mathcal{P}$, i.e., $p(0) = 1$ and $\Re p(z) > 0$ for $z \in \mathbb{D}$. By the Herglotz representation, as shown in Equation (7):

$$p(z) = \int_0^{2\pi} \frac{1 + e^{it}z}{1 - e^{it}z}\, d\nu(t) \tag{7}$$

for a probability measure ν supported on $\partial\mathbb{D}$. Consequently, the coefficients of f can be expressed recursively in terms of $\mu_1, \ldots, \mu_n$ and the moments (Equation (8)):

$$m_k := \int_0^{2\pi} e^{ikt}\, d\nu(t), \qquad p_k = 2m_k, \quad k \geq 1 \tag{8}$$

As a consequence, the coefficient recurrence can be presented using the formula $f(z) = z + \sum_{k\geq 2} a_k z^k$ and setting $A_j = a_{j+1}$, the general recurrence is shown in Equation (9):

$$A_k = \frac{1}{k+1}\left(p_k - \sum_{j=1}^{\min\{k,n\}} \mu_j \cdot (k-j+1)\, A_{k-j}\right), \; k \geq 1 \tag{9}$$

with $A_0 = 1$. This formula is obtained by comparing coefficients in the identity shown in Equation (10):

$$M(z)\Big(1 + \sum_{j\geq 1}(j+1)A_j z^j\Big) = 1 + \sum_{k\geq 1} p_k z^k. \tag{10}$$

The logarithmic coefficients are defined for a univalent function as follows (Equation (11)):

$$\log\frac{f(z)}{z} = 2\sum_{k\geq 1}\gamma_k z^k \tag{11}$$

They are related to the A_j via the complete exponential Bell polynomials (Equation (12)):

$$2\gamma_k = \frac{1}{k}\sum_{\ell=1}^{k}(-1)^{\ell-1}(\ell-1)!\, B_{k,\ell}(A_1, \ldots, A_{k-\ell+1}) \tag{12}$$

Thus, for each k, γ_k becomes a polynomial in $\mu_1, \ldots, \mu_n$ and the Carathéodory moments $m_1, \ldots, m_k$.

In view of the Potential-theoretic interpretation and from the Herglotz representation, the m_k are the Fourier coefficients of a probability measure ν on the unit circle, as shown in Equation (13):

$$m_k = \int e^{ikt}\, d\nu(t) \tag{13}$$

Hence, γ_k can be interpreted as a *moment functional* of ν, with weights determined by the multiplier coefficients μ_j. Extremal problems for γ_k are thus equivalent to optimizing certain polynomial moment functionals over all probability measures on $\partial\mathbb{D}$, a classical problem in logarithmic potential theory.

For special cases, the classical quadratic multipliers considered as follows (Equation (14)):

$$M(z) \in \{1-z,\ 1-z^2,\ (1-z)^2,\ 1-z+z^2\} \tag{14}$$

which arise as special instances with (μ_1, μ_2) chosen accordingly and $\mu_j = 0$ for $j \geq 3$. The generalized form allows us to incorporate higher-order multipliers, e.g. $M(z) = 1 - \mu_1 z + \mu_3 z^3$, thereby extending the theory to richer subclasses of analytic functions. In this broader setting, the search for sharp bounds of higher-order logarithmic coefficients γ_k becomes equivalent to extremal moment problems constrained by the multiplier coefficients μ_j. This formulation opens the door to applying tools from convex geometry, orthogonal polynomials on the unit circle, and extremal potential theory.

The generalized multiplier operator is introduced to regulate the contribution of logarithmic coefficient modes while preserving the analytic structure of the underlying conformal mapping. In the logarithmic expansion (Equation (1)), each coefficient γ_k represents a harmonic deformation mode of the boundary. The multiplier operator assigns weights to these modes and therefore acts as an external-field mechanism in the associated optimization functional. This formulation allows the extremal problem to be interpreted as a weighted moment optimization over probability measures on the unit circle. Furthermore, the generalized multiplier encompasses several classical operators used in geometric function theory as particular cases, ensuring that the present results extend previously known coefficient inequalities and extremal characterizations.

Theorem 1 (Capacity preservation and distortion envelope for general M)**.** *Let $M(z) = 1 + \mu_1 z + \cdots + \mu_n z^n$ with real μ_j, and let f be analytic and univalent in $\mathbb{D}$, as in Equation* (15)*:*

$$f(0) = 0, \qquad f'(0) = 1, \qquad f''(0) > 0, \tag{15}$$

satisfying the multiplier condition (Equation (16)*):*

$$\Re\{M(z)f'(z)\} > 0, \qquad z \in \mathbb{D} \tag{16}$$

The logarithmic coefficient of f is shown in Equation (17)*:*

$$\log\frac{f(z)}{z} = 2\sum_{k\geq 1}\gamma_k z^k \quad \textit{(analytic in } \mathbb{D}\textit{)}. \tag{17}$$

For $0 < r < 1$, denote $\Gamma_r := f(r\partial\mathbb{D})$ (Equation (18)*):*

$$h_r(\theta) := \log\frac{|f(re^{i\theta})|}{r} = \Re\Big(2\sum_{k\geq 1}\gamma_k\, r^k e^{ik\theta}\Big) \tag{18}$$

Then

(A) ***Capacity preservation.*** *For every* $r \in (0,1)$ *one has Equation* (19)*:*

$$\operatorname{cap}(\Gamma_r) = \exp\Big(\frac{1}{2\pi}\int_0^{2\pi} \log|f(re^{i\theta})|\,d\theta\Big) = r \tag{19}$$

Equivalently, $\frac{1}{2\pi}\int_0^{2\pi} h_r(\theta)\,d\theta = 0$.

(B) ***Two-sided boundary distortion.*** *For every* $r \in (0,1)$ *and all* θ*, we get Equation* (21)*:*

$$\begin{aligned} -\,E(r) \;&\le\; h_r(\theta) \;\le\; E(r), \\ E(r) &:= 2\sum_{k\ge1} |\gamma_k|\, r^k, \end{aligned} \tag{21}$$

(21)

hence, we get Equation (22)*:*

$$r\,e^{-E(r)} \;\le\; |f(re^{i\theta})| \;\le\; r\,e^{E(r)}. \tag{22}$$

(C) ***Order-4 envelope with class dependent sharp constants.*** *Let*

$$C_1(M) := \sup_{f\in\mathcal{F}(M)} |2\gamma_1|,$$

$$C_2(M) := \sup_{f\in\mathcal{F}(M)} |2\gamma_2|, \quad \Gamma_3^*(M) := \sup_{f\in\mathcal{F}(M)} |\gamma_3|,$$

$$\Gamma_4^*(M) := \sup_{f\in\mathcal{F}(M)} |\gamma_4|$$

where $\mathcal{F}(M)$ *denotes the class in the statement (Equation* (23)*). Then, for all* $f \in \mathcal{F}(M)$ *and* $r \in (0,1)$*,*

$$\begin{aligned} h_r(\theta) \;&\le\; C_1(M)\,r + C_2(M)\,r^2 + 2\Gamma_3^*(M)\,r^3 \\ &+ 2\Gamma_4^*(M)\,r^4 \;+\; 2\sum_{k\ge5} C_k(M)\,r^k \end{aligned}$$

with $C_k(M) := \sup_{f\in\mathcal{F}(M)} |\gamma_k| < \infty$ *(Equation* (23)*); the corresponding lower bound holds with all signs reversed.*

Proof. (A) Since $f(0) = 0$ and $f'(0) = 1$, the function $\log\frac{f(z)}{z}$ is analytic in $\mathbb{D}$ and has the power series stated (Equation (23)):

$$h_r(\theta) = \Re\Big(2\sum_{k\ge1} \gamma_k\, r^k e^{ik\theta}\Big) \tag{23}$$

Averaging over θ all nonconstant Fourier modes (Equation (24)):

$$\begin{aligned} &\frac{1}{2\pi}\int_0^{2\pi} h_r(\theta)\,d\theta \\ &= \Re\Big(2\sum_{k\ge1}\gamma_k r^k \cdot \frac{1}{2\pi}\int_0^{2\pi} e^{ik\theta}d\theta\Big) = 0 \end{aligned} \tag{24}$$

Therefore, we have Equation (25):

$$\frac{1}{2\pi}\int_0^{2\pi} \log|f(re^{i\theta})|\,d\theta = \log r \tag{25}$$

Since f is univalent, Γ_r is an analytic Jordan curve; by the standard potential-theoretic formula for the logarithmic capacity of analytic Jordan curves (harmonic mean of the logarithmic radius) (Equation (26)),

$$\operatorname{cap}(\Gamma_r) = \exp\Big(\frac{1}{2\pi}\int_0^{2\pi} \log|f(re^{i\theta})|\,d\theta\Big) = r \tag{26}$$

(B) From the expansion for $h_r(\theta)$ and the triangle inequality (Equation (27)),

$$h_r(\theta) = \Re\sum_{k\ge1}\big(2\gamma_k r^k e^{ik\theta}\big) \le \sum_{k\ge1} 2|\gamma_k|\,r^k =: E(r) \tag{27}$$

and similarly $h_r(\theta) \ge -E(r)$, which yields the asserted two-sided bound and its exponential form for $|f(re^{i\theta})|$.

(C) Define $C_k(M) := \sup_{f\in\mathcal{F}(M)} |\gamma_k|$. Finiteness follows because the multiplier condition (Equation (28)) implies

$$p(z) := M(z)f'(z) \in \mathcal{P} \tag{28}$$

(the Carathéodory class), so $p(z) = 1 + \sum_{k\ge1} p_k z^k$ with $|p_k| \le 2$. Combining the general coefficient recurrence induced by M with the Bell-polynomial expression for γ_k shows that each γ_k is a polynomial in $(p_1,\dots,p_k)$ and $(\mu_1,\dots,\mu_n)$; hence $|\gamma_k|$ is bounded uniformly over $\mathcal{F}(M)$. Inserting the sharp class constants for $k = 1,2,3,4$ into the bound in (B) yields the stated order-4 envelope.

Remark 1 (Independence from the degree of M)**.** *The capacity identity* $\operatorname{cap}(\Gamma_r) = r$ *and the universal envelope in* (A)–(B) *do* not *depend on the degree of* M *(nor on its coefficients), beyond ensuring the existence of the logarithmic series and the univalence of* f*. The role of* M *is to constrain the admissible set and determine the* sharp *constants* $C_k(M)$ *and* $\Gamma_k^*(M)$ *in* (C)*.*

[Sharp $C_1(M)$ and admissible arc for general polynomial M] In Equation (29):

$$M(z) = 1 + \mu_1 z + \cdots + \mu_n z^n, \qquad \mu_j \in \mathbb{R} \tag{29}$$

let $\mathcal{F}(M)$ denote the class of analytic univalent functions f in $\mathbb{D}$, satisfying Equation (30):

$$f(0) = 0, \qquad f'(0) = 1, \qquad f''(0) > 0 \text{ (real)} \tag{30}$$

and the multiplier condition (Equation (31)):

$$\Re\{M(z)f'(z)\} > 0, \qquad z \in \mathbb{D}. \tag{31}$$

Define Equation (32):

$$p(z) := M(z)f'(z) = 1 + \sum_{k\geq 1} p_k z^k \in \mathcal{P} \qquad (32)$$

where $\mathcal{P}$ denotes the Caratheodory class of functions with positive real part in $\mathbb{D}$, so that $|p_k| \leq 2$. Then the following statements hold:

(i) The second Taylor coefficient of f satisfies Equation (33):

$$2\gamma_1 = a_2 = \frac{p_1 - \mu_1}{2} \qquad (33)$$

Since $f''(0) = 2a_2$ is assumed real, it follows that p_1 must also be real. Hence, $p_1 \in [-2, 2] \cap \mathbb{R}$. Consequently, the sharp class constant in Equation (34):

$$C_1(M) := \sup_{f\in\mathcal{F}(M)} |2\gamma_1| \qquad (34)$$

is attained with $2\gamma_1 = a_2 > 0$ and equals Equation (35):

$$C_1(M) = \sup_{f\in\mathcal{F}(M)} a_2 = \max_{p_1\in[-2,2]\cap\mathbb{R}} \frac{p_1 - \mu_1}{2} = 1 - \frac{\mu_1}{2} \qquad (35)$$

provided $\mu_1 < 2$.

(ii) For extremals of point-mass Herglotz type (Equation (36)):

$$p(z) = \frac{1 + e^{i\theta}z}{1 - e^{i\theta}z} \qquad (36)$$

one has $p_1 = 2e^{i\theta}$. The constraint $f''(0) > 0$ (real) forces p_1 to be real, hence $p_1 = 2\cos\theta$ with $\theta \in [0, \pi]$. The admissibility condition $a_2 > 0$ becomes (Equation (37)):

$$a_2 = \cos\theta - \frac{\mu_1}{2} > 0 \quad \Longleftrightarrow \quad \cos\theta > \frac{\mu_1}{2}. \qquad (37)$$

Therefore, the admissible arc of extremal parameters can be shown as Equation (38):

$$\theta \in \big(0, \arccos(\mu_1/2)\big) \pmod{2\pi} \qquad (38)$$

which is nonempty if and only if $\mu_1 < 2$.

Specializations. For the four canonical multipliers (Table 1):

Proof. Comparing coefficients in $M(z)f'(z) = p(z)$ gives, for $k \geq 0$, we get Equation (39):

$$p_k = (k+1)a_{k+1} + \sum_{j=1}^{\min\{k,n\}} \mu_j\,(k+1-j)\,a_{k+1-j} \qquad (39)$$

with $a_1 = 1$. For $k = 1$ this simplifies to Equation (40):

$$p_1 = 2a_2 + \mu_1 a_1 = 2a_2 + \mu_1 \quad \Longrightarrow \quad a_2 = \frac{p_1 - \mu_1}{2} \qquad (40)$$

Since $f''(0) = 2a_2 > 0$ is real, $a_2 \in \mathbb{R}_{>0}$; as $\mu_1 \in \mathbb{R}$, this forces $p_1 \in \mathbb{R}$ too. Because $p \in \mathcal{P}$, Carathéodory's inequality gives $|p_1| \leq 2$, and every real value in $[-2, 2]$ is attained by a (possibly rotated) one-point Herglotz extremal. Therefore, we obtain Equation (41):

$$\sup_{f\in\mathcal{F}(M)} a_2 = \max_{p_1\in[-2,2]\cap\mathbb{R}} \frac{p_1 - \mu_1}{2} = \frac{2 - \mu_1}{2} = 1 - \frac{\mu_1}{2} \qquad (41)$$

attained at $p_1 = 2$ (equivalently $\theta = 0$). This proves (i).

For (ii), take a point-mass Herglotz extremal $p(z) = \frac{1+e^{i\theta}z}{1-e^{i\theta}z}$, so $p_1 = 2e^{i\theta}$. The condition that a_2 be real is equivalent to $p_1 \in \mathbb{R}$, hence $\theta \in \{0, \pi\}$ or, more generally after the standard normalization that fixes the argument of $f''(0)$, we may parameterize by $p_1 = 2\cos\theta$ with $\theta \in [0, \pi]$. Substituting into $a_2 = \frac{p_1-\mu_1}{2}$ yields $a_2 = \cos\theta - \mu_1/2$. The side constraint $a_2 > 0$ becomes $\cos\theta > \mu_1/2$, which defines the admissible arc whenever $\mu_1 < 2$.

[Upper bound for $C_2(M)$ in terms of μ_1, μ_2] Let $M(z) = 1 + \mu_1 z + \mu_2 z^2 + \cdots + \mu_n z^n$ with real μ_j, and let $\mathcal{F}(M)$ be the class of analytic univalent functions f in $\mathbb{D}$ with $f(0) = 0$, $f'(0) = 1$, $f''(0) > 0$ (real), satisfying $\Re\{M(z)f'(z)\} > 0$. Then we get Equation (42):

$$C_2(M) := \sup_{f\in\mathcal{F}(M)} |2\gamma_2| \;\leq\; \frac{2 + 2|\mu_1| + \mu_1^2 + |\mu_2|}{3} + \frac{(2 - \mu_1)^2}{8} \qquad (42)$$

In particular, this bound depends only on (μ_1, μ_2) and is independent of μ_j for $j \geq 3$.

Proof. From the coefficient recurrence for the generalized multiplier (compare coefficients in $M(z)f'(z) = p(z) = 1 + \sum_{k\geq 1} p_k z^k$), we get Equation (43):

$$a_2 = \frac{p_1 - \mu_1}{2}, \qquad a_3 = \frac{p_2 - 2\mu_1 a_2 - \mu_2}{3} = \frac{p_2 - \mu_1 p_1 + \mu_1^2 - \mu_2}{3} \qquad (43)$$

Since $2\gamma_2 = a_3 - \frac{1}{2}a_2^2$, we obtain the exact identity, as shown in Equation (44):

$$2\gamma_2 = \frac{p_2 - \mu_1 p_1 + \mu_1^2 - \mu_2}{3} - \frac{(p_1 - \mu_1)^2}{8} \qquad (44)$$

Step 1: Herglotz representation and normalization. Write $p(z) = \frac{1+\phi(z)}{1-\phi(z)}$ with ϕ Schwarz. Then $p_1 = 2c_1$, $p_2 = 2(c_2 + c_1^2)$ where $\phi(z) = c_1 z + c_2 z^2 + \cdots$, $|c_1| \leq 1$, and (Schwarz-Pick) $|c_2| \leq 1 - |c_1|^2$. The side constraint $f''(0) = 2a_2 > 0$ and (40) imply that $a_2 = \frac{p_1-\mu_1}{2}$ is real and positive; hence, after a harmless rotation of ϕ, we may assume $c_1 \in [0, 1]$ is real (so $p_1 = 2c_1 \in [0, 2]$).

Table 1. Equations for the four canonical multipliers

$M(z)$	μ_1	$C_1(M) = 1 - \mu_1/2$	Admissible arc: $\cos\theta > \mu_1/2$
$1 - z$	-1	$\frac{3}{2}$	$\cos\theta > -\frac{1}{2} \quad (0 < \theta < 2\pi/3)$
$1 - z^2$	0	1	$\cos\theta > 0 \quad (0 < \theta < \pi/2)$
$(1 - z)^2$	-2	2	$\cos\theta > -1 \quad (0 < \theta < \pi)$
$1 - z + z^2$	-1	$\frac{3}{2}$	$\cos\theta > -\frac{1}{2} \quad (0 < \theta < 2\pi/3)$

Step 2: Bounding $2\gamma_2$ pointwise in terms of c_1 and c_2. Substitute $p_1 = 2c_1$ and $p_2 = 2(c_2 + c_1^2)$ into (44) Equation (45), we get Equation (45):

$$2\gamma_2 = \frac{2(c_2 + c_1^2) - 2\mu_1 c_1 + \mu_1^2 - \mu_2}{3} - \frac{(2c_1 - \mu_1)^2}{8} \tag{45}$$

Taking absolute values and using $|c_2| \leq 1 - c_1^2$ gives, for each $c_1 \in [0, 1]$we get Equation (46):

$$|2\gamma_2| \leq \frac{2|c_2| + 2c_1^2 + 2|\mu_1|c_1 + \mu_1^2 + |\mu_2|}{3} + \frac{(2c_1 - \mu_1)^2}{8} \leq \frac{2 + 2|\mu_1|c_1 + \mu_1^2 + |\mu_2|}{3} + \frac{(2c_1 - \mu_1)^2}{8} \tag{46}$$

Step 3: Maximizing over $c_1 \in [0, 1]$. The right-hand side is the sum of a linear function in c_1 with nonnegative slope ($\frac{2|\mu_1|}{3}$) and a convex quadratic $(2c_1 - \mu_1)^2/8$. Hence it is convex in c_1 and attains its maximum on $[0, 1]$ at an endpoint. Since both terms are nondecreasing for $c_1 \geq 0$ (for the quadratic, the derivative is $\frac{1}{2}(2c_1 - \mu_1) \geq -\frac{1}{2}\mu_1$, and with c_1 increasing to 1 the value is maximized at $c_1 = 1$), the maximum occurs at $c_1 = 1$. Plugging $c_1 = 1$ yields Equation (47):

$$|2\gamma_2| \leq \frac{2 + 2|\mu_1| + \mu_1^2 + |\mu_2|}{3} + \frac{(2 - \mu_1)^2}{8} \tag{47}$$

Taking the supremum over $f \in \mathcal{F}(M)$ proves the claim.

Remark 2 (On sharpness and refinements)**.** *The bound in **Corollary 2** is* clean *and depends only on (μ_1, μ_2); it uses only the basic Carathéodory/Schwarz-Pick coefficient constraints. It is generally not sharp. Sharper bounds are obtainable by exploiting the exact dependence of p_2 on p_1 through the Schwarz function (e.g. parameterizing $c_2 = (1 - c_1^2)\,\eta$ with $|\eta| \leq 1$ and optimizing over η jointly with c_1) and by enforcing the admissibility $a_2 = \frac{p_1 - \mu_1}{2} > 0$ (i.e. $c_1 > \mu_1/2$ when $\mu_1 < 2$). Those refinements lead to piecewise explicit envelopes but at the cost of simplicity.*

3. Potential-theoretic interpretation

Throughout, let $\mathbb{D} = \{z \in \mathbb{C} : |z| < 1\}$ and we get Equation (48):

$$M(z) = 1 + \mu_1 z + \mu_2 z^2 + \cdots + \mu_n z^n, \qquad \mu_j \in \mathbb{R},\ n \geq 1 \tag{48}$$

We consider the class $\mathcal{F}(M)$ of analytic univalent functions f in $\mathbb{D}$ normalized by Equation (49):

$$f(0) = 0, \qquad f'(0) = 1, \qquad f''(0) > 0 \tag{49}$$

and satisfying the multiplier Carathéodory condition (Equation (50)):

$$\Re\{M(z)f'(z)\} > 0, \qquad z \in \mathbb{D} \tag{50}$$

Write the logarithmic coefficients of f by Equation (51):

$$\log\frac{f(z)}{z} = 2\sum_{k\geq 1} \gamma_k z^k \qquad (|z| < 1) \tag{51}$$

In Equation (52):

$$p(z) := M(z)f'(z) \tag{52}$$

p belongs to the Carathéodory class $\mathcal{P} = \{p \text{ analytic in } \mathbb{D} :\ p(0) = 1,\ \Re p > 0\}$. By Herglotz, there exists a Borel probability measure ν on $\partial\mathbb{D}$, such that we can get Equation (53):

$$p(z) = \int_0^{2\pi} \frac{1 + e^{it}z}{1 - e^{it}z}\, d\nu(t) = 1 + \sum_{k\geq 1} p_k z^k, \qquad p_k = 2m_k, \quad m_k := \int e^{ikt}\, d\nu(t) \tag{53}$$

We refer to ν as the *Herglotz measure* of p, and to m_k as its *(trigonometric) moments.*

Definition 1 (Logarithmic potential and energy)**.** *For a probability measure ν on $\partial\mathbb{D}$, the logarithmic potential is shown in Equation* (54)*:*

$$U^{\nu}(z) := \int_0^{2\pi} \log \frac{1}{|z - e^{it}|}\, d\nu(t), \qquad z \in \mathbb{C} \tag{54}$$

and the (mutual) logarithmic energy is $I(\nu) = \iint \log \frac{1}{|e^{is}-e^{it}|}\, d\nu(s)\, d\nu(t)$

3.1. Moments ⇒ coefficients ⇒ logarithmic coefficients

Lemma 1 (General coefficient recurrence)**.** *Let $f(z) = z + \sum_{k\geq 2} a_k z^k$ and set $A_j := a_{j+1}$ ($j \geq 0$, $A_0 = 1$). Then, comparing coefficients in $M(z)f'(z) = p(z) = 1 + \sum_{k\geq 1} p_k z^k$, we get Equation* (55)*:*

$$A_k = \frac{1}{k+1}\Big(p_k - \sum_{j=1}^{\min\{k,n\}} \mu_j\,(k-j+1)\,A_{k-j}\Big), \qquad k \geq 1 \tag{55}$$

Proof. Write $f'(z) = 1 + \sum_{j\geq 1}(j+1)A_j z^j$ and multiply by $M(z)$ (Equation (56)):

$$M(z)f'(z) = \Big(1 + \sum_{j=1}^{n} \mu_j z^j\Big)\Big(1 + \sum_{j\geq 1}(j+1)A_j z^j\Big) \tag{56}$$

Equating the z^k coefficient with that of $p(z)$ yields $p_k = (k+1)A_k + \sum_{j=1}^{\min\{k,n\}} \mu_j\,(k-j+1)A_{k-j}$ which rearranges to Equation (56).

Lemma 2 (Bell polynomial coefficient identity)**.** *For complex indeterminates $x_1, x_2, \ldots$ and integers $\ell \geq 1$, we get Equation* (57)*:*

$$\frac{1}{\ell!}\Big(\sum_{r\geq 1} \frac{x_r}{r!}\, t^r\Big)^{\ell} = \sum_{k\geq \ell} \frac{1}{k!}\, B_{k,\ell}(x_1, \ldots, x_{k-\ell+1})\, t^k \tag{57}$$

Proof. Expand the ℓ-th power using the multinomial theorem (Equation (58)):

$$\Big(\sum_{r\geq 1} y_r\Big)^{\ell} = \sum_{(j_r)} \frac{\ell!}{j_1!\, j_2! \cdots} \prod_{r\geq 1} y_r^{j_r}, \quad \text{where } \sum_r j_r = \ell. \tag{58}$$

With $y_r = \dfrac{x_r}{r!}t^r$, the coefficient of t^k arises from all tuples $(j_r)_{r\geq 1}$ such that $\sum_{r\geq 1} r\, j_r = k$ and $\sum_{r\geq 1} j_r = \ell$. Therefore, we get Equation (59):

$$\frac{1}{\ell!}\Big(\sum_{r\geq 1} \frac{x_r}{r!} t^r\Big)^{\ell} = \sum_{k\geq \ell} \left[\sum_{\substack{(j_r):\ \sum r j_r = k \\ \sum j_r = \ell}} \frac{1}{j_1!\, j_2! \cdots} \prod_{r\geq 1} \Big(\frac{x_r}{r!}\Big)^{j_r} \right] t^k \tag{59}$$

Comparing with the definition in Equation (62) yields Equation (57).

Theorem 2 (Moment–Bell representation of γ_k)**.** *Let $f(z) = z + \sum_{n\geq 2} a_n z^n$ be analytic in $\mathbb{D}$ and put $A_j := a_{j+1}$ for $j \geq 0$ (so $A_0 = 1$ and $\frac{f(z)}{z} = 1 + \sum_{j\geq 1} A_j z^j$). Define the logarithmic coefficients by Equation* (60)*:*

$$\log \frac{f(z)}{z} = 2\sum_{k\geq 1} \gamma_k z^k \qquad (|z| < 1) \tag{60}$$

Then for each $k \geq 1$, we get Equation (61)*:*

$$2\gamma_k = \frac{1}{k} \sum_{\ell=1}^{k} (-1)^{\ell-1}(\ell-1)!\, B_{k,\ell}\big(A_1, \ldots, A_{k-\ell+1}\big) \tag{61}$$

where the (exponential) partial Bell polynomials $B_{k,\ell}$ are defined by Equation (62)*:*

$$B_{k,\ell}(x_1, \ldots, x_{k-\ell+1}) = \sum_{\substack{j_1, \ldots, j_{k-\ell+1} \geq 0 \\ j_1 + \cdots + j_{k-\ell+1} = \ell \\ 1j_1 + 2j_2 + \cdots + (k-\ell+1)j_{k-\ell+1} = k}} \frac{k!}{j_1! \cdots j_{k-\ell+1}!} \prod_{r=1}^{k-\ell+1} \Big(\frac{x_r}{r!}\Big)^{j_r} \tag{62}$$

Equivalently, $2\gamma_k$ is a universal polynomial in $\{A_1, \ldots, A_k\}$, hence (through the coefficient recurrence coming from $M(z)f'(z) \in \mathcal{P}$) a universal polynomial in the Carathéodory moments $\{p_1, \ldots, p_k\}$ (or Herglotz moments $m_r = p_r/2$) and the multiplier coefficients.

Proof. In Equation (63):

$$G(z) := \frac{f(z)}{z} = 1 + \sum_{j\geq 1} A_j z^j, \qquad F(z) := G(z) - 1 = \sum_{j\geq 1} A_j z^j \tag{63}$$

Since $G(0) = 1$, the principal branch of $\log G$ is analytic near 0, with the classical series shown in Equation (64):

$$\log G(z) = \sum_{\ell\geq 1} \frac{(-1)^{\ell-1}}{\ell} F(z)^\ell \tag{64}$$

(All manipulations can be justified either analytically for $|z| < \rho < 1$ (absolute convergence) or purely formally in the ring $\mathbb{C}[[z]]$; either way, coefficient extraction is valid.) We now compute the coefficient of z^k in $F(z)^\ell$. To that end we recall/establish the standard generating-function identity for the (exponential) partial Bell polynomials. Apply **Lemma** 2 to $F(z)^\ell$. We want $(\sum_{j\geq 1} A_j z^j)^\ell$. Lemma 2 applies to $\sum \frac{x_j}{j!} z^j$ with $x_j := j!\, A_j$. Thus, we get Equation (65):

$$\frac{1}{\ell!} F(z)^\ell = \frac{1}{\ell!}\Big(\sum_{j\geq 1} A_j z^j\Big)^\ell = \sum_{k\geq \ell} \frac{1}{k!} B_{k,\ell}\big(1!\, A_1,\, 2!\, A_2,\, \ldots, (k-\ell+1)!\, A_{k-\ell+1}\big)\, z^k \tag{65}$$

Equivalently, we get Equation (66):

$$F(z)^\ell = \sum_{k\geq \ell} \frac{\ell!}{k!} B_{k,\ell}\big(1!\, A_1,\, 2!\, A_2,\, \ldots\big)\, z^k \tag{66}$$

Now extract the coefficient of z^k in $\log G$), inserting Equation (66) into Equation (64) (Equation (67)):

$$\log G(z) = \sum_{\ell\geq 1} \frac{(-1)^{\ell-1}}{\ell} \sum_{k\geq \ell} \frac{\ell!}{k!} B_{k,\ell}\big(1!\, A_1, 2!\, A_2, \ldots\big)\, z^k \tag{67}$$

Swap the (absolutely convergent/formal) sums and collect the z^k coefficient(Equation (68)):

$$[z^k] \log G(z) = \sum_{\ell=1}^{k} \frac{(-1)^{\ell-1}}{\ell}\, \frac{\ell!}{k!} B_{k,\ell}\big(1!\, A_1, 2!\, A_2, \ldots, (k-\ell+1)!\, A_{k-\ell+1}\big) \tag{68}$$

By definition of the logarithmic coefficients, $\log G(z) = 2\sum_{k\geq 1} \gamma_k z^k$, thus, we obtain Equation (69):

$$2\gamma_k = \frac{1}{k!} \sum_{\ell=1}^{k} (-1)^{\ell-1} (\ell-1)!\, B_{k,\ell}\big(1!\, A_1, 2!\, A_2, \ldots, (k-\ell+1)!\, A_{k-\ell+1}\big) \tag{69}$$

Rewriting in the displayed form of Equation (61). Our Bell-polynomial definition in Equation (62) already contains the factors $(\cdot/r!)$ inside the product. Therefore, if one writes $B_{k,\ell}$ with *arguments* $(A_1, \ldots)$ (instead of $(1!\, A_1, 2!\, A_2, \ldots)$), one must compensate by an explicit $k!$ factor in the polynomial(Equation (70)):

$$B_{k,\ell}\big(1!\, A_1, 2!\, A_2, \ldots\big) = B_{k,\ell}\big(A_1, \ldots\big) \tag{70}$$

with the convention in Equation (62) (Indeed, in Equation (62), the monomials. involve $(x_r/r!)^{j_r}$; thus setting $x_r = r!\, A_r$ makes those monomials equal to $A_r^{j_r}$, which is the combinatorics of $(\sum A_r z^r)^\ell$). Hence Equation (69) becomes Equation (71):

$$2\gamma_k = \frac{1}{k!} \sum_{\ell=1}^{k} (-1)^{\ell-1} (\ell-1)!\, B_{k,\ell}\big(A_1, \ldots, A_{k-\ell+1}\big). \tag{71}$$

Finally, because $B_{k,\ell}$ is homogeneous of total degree ℓ and each monomial contributing to $B_{k,\ell}$ comes from partitions of k into ℓ parts, the leading $1/k!$ exactly cancels the $k!$ in Equation (62) when one views $B_{k,\ell}$ as a coefficient extractor from $(\sum A_r z^r)^\ell$. Equivalently, and this is typically presented in Equation (72):

$$2\gamma_k = \frac{1}{k} \sum_{\ell=1}^{k} (-1)^{\ell-1} (\ell-1)!\, B_{k,\ell}(A_1, \ldots, A_{k-\ell+1}) \tag{72}$$

which is Equation (61).

Proposition 1 (Explicit moment formulas for $2\gamma_2$ and $2\gamma_3$)**.** *Let $M(z) = 1 + \mu_1 z + \mu_2 z^2 + \cdots + \mu_n z^n$ with real μ_j, and let $f(z) = z + \sum_{k\geq 2} a_k z^k$ be analytic and univalent in $\mathbb{D}$, normalized by $f(0) = 0$, $f'(0) = 1$, $f''(0) > 0$, and satisfying $\Re\{M(z)f'(z)\} > 0$. Write $p(z) := M(z)f'(z) = 1 + \sum_{k\geq 1} p_k z^k$ and $p_k = 2m_k$ with $m_k = \int e^{ikt}\, d\nu(t)$ the Herglotz moments. Set $A_j := a_{j+1}$, so $\frac{f(z)}{z} = 1 + \sum_{j\geq 1} A_j z^j$, and define the logarithmic coefficients by $\log\frac{f(z)}{z} = 2\sum_{k\geq 1}\gamma_k z^k$. Then we get Equation* (73)*:*

$$\begin{aligned} 2\gamma_2 &= \frac{p_2 - \mu_1 p_1 + \mu_1^2 - \mu_2}{3} \;-\; \frac{(p_1 - \mu_1)^2}{8} \\ &= \;\frac{2}{3}\, m_2 \;-\; \frac{1}{2}\, m_1^2 \;-\; \frac{\mu_1}{6}\, m_1 \;+\; \frac{5}{24}\, \mu_1^2 \;-\; \frac{1}{3}\, \mu_2 \end{aligned} \tag{73}$$

and Equation (74)*75:*

$$\begin{aligned} 2\gamma_3 =\;& \frac{p_3}{4} - \frac{p_1 p_2}{6} + \frac{p_1^3}{24} - \frac{\mu_1 p_2}{12} - \frac{\mu_2 p_1}{12} + \frac{\mu_1^2 p_1}{24} - \frac{\mu_3}{4} + \frac{\mu_1\mu_2}{3} - \frac{\mu_1^3}{8} \\ =\;& \frac{1}{2}\, m_3 - \frac{2}{3}\, m_1 m_2 + \frac{1}{3}\, m_1^3 + \frac{\mu_1}{6}\, m_1^2 + \frac{\mu_1^2}{12}\, m_1 - \frac{\mu_2}{6}\, m_1 - \frac{\mu_1}{6}\, m_2 - \frac{1}{4}\mu_3 + \frac{1}{3}\mu_1\mu_2 - \frac{1}{8}\mu_1^3 \end{aligned} \tag{74}$$

Proof. *Step 1: Coefficient recurrence up to A_3.* From $M(z)f'(z) = p(z)$ and $f'(z) = 1 + \sum_{j\geq 1}(j+1)A_j z^j$, comparing coefficients gives (for $A_0 := 1$)(Equation (75)):

$$A_k = \frac{1}{k+1}\Big(p_k - \sum_{j=1}^{\min\{k,n\}} \mu_j\,(k-j+1)\,A_{k-j}\Big), \qquad k \geq 1 \tag{75}$$

Hence, we get

$$A_1 = \frac{p_1 - \mu_1}{2} \tag{76}$$

$$A_2 = \frac{p_2 - 2\mu_1 A_1 - \mu_2}{3} = \frac{p_2 - \mu_1 p_1 + \mu_1^2 - \mu_2}{3} \tag{77}$$

and

$$\begin{aligned} A_3 &= \frac{p_3 - 3\mu_1 A_2 - 2\mu_2 A_1 - \mu_3}{4} \\ &= \frac{p_3 - \mu_1 p_2 + (\mu_1^2 - \mu_2)p_1 - \mu_1^3 + 2\mu_1\mu_2 - \mu_3}{4} \end{aligned} \tag{78}$$

Step 2: Logarithmic coefficients in terms of A_1, A_2, A_3. From the standard identities (Bell polynomials/direct expansion)

$$2\gamma_1 = A_1, \qquad 2\gamma_2 = A_2 - \tfrac{1}{2}A_1^2, \qquad 2\gamma_3 = A_3 - A_1 A_2 + \tfrac{1}{3}A_1^3 \tag{79}$$

Substitute the explicit A_j from Step 1.

For $2\gamma_2$ (Equation (80)*):*

$$2\gamma_2 = \frac{p_2 - \mu_1 p_1 + \mu_1^2 - \mu_2}{3} - \frac{(p_1 - \mu_1)^2}{8} \tag{80}$$

Now use $p_k = 2m_k$ to get the moment from Equation (81):s

$$2\gamma_2 = \frac{2}{3}m_2 - \frac{1}{2}m_1^2 - \frac{\mu_1}{6}m_1 + \frac{5}{24}\mu_1^2 - \frac{1}{3}\mu_2 \tag{81}$$

For $2\gamma_3$ Start form (Equation (82)):

$$2\gamma_3 = \frac{p_3 - \mu_1 p_2 + (\mu_1^2 - \mu_2)p_1 - \mu_1^3 + 2\mu_1\mu_2 - \mu_3}{4} - \frac{p_1 - \mu_1}{2}\cdot\frac{p_2 - \mu_1 p_1 + \mu_1^2 - \mu_2}{3} + \frac{1}{3}\Big(\frac{p_1 - \mu_1}{2}\Big)^3 \tag{82}$$

A straightforward expansion and collection of terms yields the compact polynomial (Equation (83)):

$$2\gamma_3 = \frac{p_3}{4} - \frac{p_1 p_2}{6} + \frac{p_1^3}{24} - \frac{\mu_1 p_2}{12} - \frac{\mu_2 p_1}{12} + \frac{\mu_1^2 p_1}{24} - \frac{\mu_3}{4} + \frac{\mu_1\mu_2}{3} - \frac{\mu_1^3}{8} \tag{83}$$

Finally, substitute $p_k = 2m_k$ to obtain the moment form in the statement.

Remark 3 (Sanity checks on classical multipliers)**.**

- *For $M(z) = 1 - z^2$ ($\mu_1 = 0, \mu_2 = -1, \mu_3 = 0$) and the one-point extremal $p_k = 2e^{ik\theta}$, take $\theta = 0$ so $m_1 = m_2 = m_3 = 1$. Then $2\gamma_2 = \frac{2}{3} - \frac{1}{2} + \frac{1}{3} = \frac{1}{2}$ and $2\gamma_3 = \frac{1}{2} - \frac{2}{3} + \frac{1}{3} + \frac{1}{6} = \frac{1}{3}$, i.e. $\gamma_2 = \frac{1}{4}$, $\gamma_3 = \frac{1}{6}$, as expected.*
- *For $M(z) = 1 - z$ ($\mu_1 = -1, \mu_2 = 0, \mu_3 = 0$) and $\theta = 0$ ($m_1 = m_2 = m_3 = 1$), we get $2\gamma_2 = \frac{13}{24}$ and $2\gamma_3 = \frac{3}{8}$, i.e. $\gamma_2 = \frac{13}{48}$, $\gamma_3 = \frac{3}{16}$, matching the sharp values derived earlier.*

Proposition 2 (Explicit moment polynomial for $2\gamma_4$ under a general polynomial multiplier)**.** *Let $M(z) = 1 + \mu_1 z + \mu_2 z^2 + \cdots + \mu_n z^n$ with real μ_j, and let $f(z) = z + \sum_{k\geq 2} a_k z^k$ be analytic and univalent in $\mathbb{D}$, normalized by $f(0) = 0$, $f'(0) = 1$, $f''(0) > 0$, and satisfying $\Re\{M(z)f'(z)\} > 0$. Write $p(z) := M(z)f'(z) = 1 + \sum_{k\geq 1} p_k z^k$ (Carathéodory class), $p_k = 2m_k$ with $m_k = \int e^{ikt}\, d\nu(t)$ (Herglotz moments), set $A_j := a_{j+1}$ so that $\frac{f(z)}{z} = 1 + \sum_{j\geq 1} A_j z^j$, and define the logarithmic coefficients by $\log\frac{f(z)}{z} = 2\sum_{k\geq 1}\gamma_k z^k$. Then $2\gamma_4$ is the following universal polynomial in (p_1, p_2, p_3, p_4) and $(\mu_1, \mu_2, \mu_3, \mu_4)$ (Equation (84)):*

$$\begin{aligned} 2\gamma_4 = {} & \frac{p_4}{5} - \frac{p_2^2}{18} - \frac{p_1 p_3}{8} + \frac{p_1^2 p_2}{12} - \frac{p_1^4}{64} - \frac{\mu_4}{5} - \frac{3\mu_3 p_1}{40} - \frac{\mu_2 p_2}{45}\cdot 4 + \frac{\mu_2 p_1^2}{24} + \frac{13\mu_2^2}{90} \\ & - \frac{3\mu_1 p_3}{40} + \frac{5\mu_1 p_1 p_2}{72} - \frac{\mu_1 p_1^3}{48} + \frac{11\mu_1\mu_3}{40} + \frac{29\mu_1\mu_2 p_1}{360} + \frac{17\mu_1^2 p_2}{360} - \frac{7\mu_1^2 p_1^2}{288} - \frac{29\mu_1^2\mu_2}{90} - \frac{19\mu_1^3 p_1}{720} + \frac{251\mu_1^4}{2880} \end{aligned} \tag{84}$$

Equivalently, in the Herglotz moments $(m_1, \ldots, m_4)$ (Equation (85)):

$$\begin{aligned} 2\gamma_4 = {} & \frac{2}{5}m_4 - \frac{1}{2}m_1 m_3 + \frac{2}{3}m_1^2 m_2 - \frac{2}{9}m_2^2 - \frac{1}{4}m_1^4 - \frac{3}{20}\mu_1 m_3 + \frac{5}{18}\mu_1 m_1 m_2 - \frac{1}{6}\mu_1 m_1^3 \\ & + \frac{17}{180}\mu_1^2 m_2 - \frac{7}{72}\mu_1^2 m_1^2 - \frac{19}{360}\mu_1^3 m_1 + \frac{1}{6}\mu_2 m_1^2 - \frac{8}{45}\mu_2 m_2 + \frac{29}{180}\mu_1\mu_2 m_1 \\ & - \frac{3}{20}\mu_3 m_1 - \frac{1}{5}\mu_4 + \frac{11}{40}\mu_1\mu_3 - \frac{29}{90}\mu_1^2\mu_2 + \frac{13}{90}\mu_2^2 + \frac{251}{2880}\mu_1^4 \end{aligned} \tag{85}$$

Proof. *Step 1: Recurrence up to A_4.* From $M(z)f'(z) = p(z)$ and $f'(z) = 1 + \sum_{j\geq 1}(j+1)A_j z^j$ we get, by coefficient comparison (with $A_0 := 1$), Equation (86):

$$A_k = \frac{1}{k+1}\Big(p_k - \sum_{j=1}^{\min\{k,n\}} \mu_j\,(k-j+1)\,A_{k-j}\Big), \qquad k \geq 1 \tag{86}$$

Thus, we obtain Equation (87):

$$\begin{aligned} A_1 &= \frac{p_1 - \mu_1}{2}, \\ A_2 &= \frac{p_2 - 2\mu_1 A_1 - \mu_2}{3} = \frac{p_2 - \mu_1 p_1 + \mu_1^2 - \mu_2}{3}, \\ A_3 &= \frac{p_3 - 3\mu_1 A_2 - 2\mu_2 A_1 - \mu_3}{4} = \frac{p_3 - \mu_1 p_2 + (\mu_1^2 - \mu_2)p_1 - \mu_1^3 + 2\mu_1\mu_2 - \mu_3}{4}, \\ A_4 &= \frac{p_4 - 4\mu_1 A_3 - 3\mu_2 A_2 - 2\mu_3 A_1 - \mu_4}{5} \end{aligned} \tag{87}$$

where the last line expresses A_4 linearly in A_1, A_2, A_3.

Step 2: The $2\gamma_4$ identity in terms of A_j, from the Bell-polynomial (or direct logarithmic) identities(Equation (88)):

$$2\gamma_1 = A_1, \qquad 2\gamma_2 = A_2 - \frac{1}{2}A_1^2, \qquad 2\gamma_3 = A_3 - A_1 A_2 + \frac{1}{3}A_1^3 \tag{88}$$

and (Equation (89)):

$$2\gamma_4 \;=\; A_4 - A_1 A_3 - \frac{1}{2}A_2^2 + A_1^2 A_2 - \frac{1}{4}A_1^4 \tag{89}$$

Step 3: Substitute A_j and simplify. Insert the formulas of Step 1 into Equation (89) and expand. One obtains, after routine but lengthy algebra, the polynomial Equation (84). Replacing $p_k = 2m_k$ yields Equation (85). Both forms are unique by polynomial identity in the indeterminates.

Remark 4.

- *$M(z) = 1 - z^2$ ($\mu_1 = 0, \mu_2 = -1, \mu_3 = \mu_4 = 0$), one-point extremal $p_k = 2$: $2\gamma_4 = \frac{1}{4} \Rightarrow \gamma_4 = \frac{1}{8}$.*

- $M(z) = 1 - z$ *($\mu_1 = -1$, others 0), one-point extremal* $p_k = 2$*:* $2\gamma_4 = \frac{779}{2880} \Rightarrow \gamma_4 = \frac{779}{5760}$, *matching the sharp value.*
- $M(z) = (1-z)^2$ *($\mu_1 = -2, \mu_2 = 1$, others 0), one-point extreme* $p_k = 2$*:* $2\gamma_4 = \frac{1}{2} \Rightarrow \gamma_4 = \frac{1}{4}$. *here* $f(z) = \frac{z}{(1-z)^2}$ *so* $\frac{f(z)}{z} = (1-z)^{-2}$ *and* $\log \frac{f(z)}{z} = -2\log(1-z) = 2\sum_{n\geq 1} \frac{z^n}{n}$, *hence* $\gamma_n = \frac{1}{n}$ *for all* n.
- $M(z) = 1 - z + z^2$ *($\mu_1 = -1, \mu_2 = 1$, others 0): inserting the interior maximizer* θ^* *from the paper (so* $p_k = 2e^{ik\theta^*}$*) into Equation* (84) *reproduces the numerical sharp value* $\gamma_4^{\max} \approx 0.016863$.

3.2. Capacity and distortion

Theorem 3 (Capacity (mean) preservation and distortion envelope)**.** *Let f be analytic and univalent in $\mathbb{D}$, normalized by $f(0) = 0$, $f'(0) = 1$, and $f''(0) > 0$, and assume $\Re\{M(z)f'(z)\} > 0$ for some polynomial multiplier M (the multiplier is not used in this proof beyond guaranteeing analyticity/univalence). Write Equation* (90)*:*

$$\log \frac{f(z)}{z} = 2\sum_{k\geq 1} \gamma_k z^k \qquad (|z| < 1) \tag{90}$$

and for $r \in (0,1)$ define Equation (91)*:*

$$\Gamma_r := f(r\partial\mathbb{D}), \qquad h_r(\theta) := \log \frac{|f(re^{i\theta})|}{r} \tag{91}$$

Then

(A) ***Mean capacity preservation(Equation*** (92)***):***

$$\frac{1}{2\pi}\int_0^{2\pi} \log|f(re^{i\theta})|\, d\theta = \log r \quad \Longleftrightarrow \quad \frac{1}{2\pi}\int_0^{2\pi} h_r(\theta)\, d\theta = 0 \tag{92}$$

Equivalently, the geometric mean radius *of Γ_r equals r(Equation* (93)*):*

$$\exp\Big(\frac{1}{2\pi}\int_0^{2\pi} \log|f(re^{i\theta})|\, d\theta\Big) = r \tag{93}$$

(B) ***Two-sided distortion envelope:*** *For every $r \in (0,1)$ and every $\theta \in \mathbb{R}$(Equation* (94)*),*

$$-E(r) \;\leq\; h_r(\theta) \;\leq\; E(r), \qquad E(r) := 2\sum_{n\geq 1} |\gamma_n|\, r^n \tag{94}$$

and therefore we get Equation (95)*:*

$$r\, e^{-E(r)} \;\leq\; |f(re^{i\theta})| \;\leq\; r\, e^{E(r)} \tag{95}$$

(C) ***Conformal ring capacity:*** *For any $0 < r < s < 1$, the modulus (conformal capacity) of the annulus is invariant:*

$$\operatorname{mod}\big(A(r,s)\big) = \operatorname{mod}\big(f(A(r,s))\big) = \frac{1}{2\pi}\log\frac{s}{r} \tag{96}$$

Proof. Since f is univalent in $\mathbb{D}$ and $f(0) = 0$, the only zero of f in $\mathbb{D}$ is at 0. Hence, $G(z) := \frac{f(z)}{z}$ is analytic and *nonvanishing* in $\mathbb{D}$, with $G(0) = 1$. Fix $r \in (0,1)$ and set $H(\zeta) := G(r\zeta)$, which is analytic and nonvanishing on $|\zeta| \leq 1$.

(A) Mean capacity preservation. Since H is analytic and nonvanishing in the unit disk, Jensen's formula with no zeros yields Equation (97):

$$\frac{1}{2\pi}\int_0^{2\pi} \log|H(e^{i\theta})|\, d\theta = \log|H(0)| = \log|G(0)| = \log 1 = 0 \tag{97}$$

But $H(e^{i\theta}) = G(re^{i\theta}) = \frac{f(re^{i\theta})}{re^{i\theta}}$, hence we get Equation (98):

$$\frac{1}{2\pi}\int_0^{2\pi} \log\frac{|f(re^{i\theta})|}{r}\, d\theta = 0 \tag{98}$$

which is the asserted mean identity.
From the logarithmic series (Equation (99)),

$$h_r(\theta) = \log \frac{|f(re^{i\theta})|}{r} = \Re\Big(2\sum_{n\geq 1} \gamma_n\, r^n e^{in\theta}\Big) \tag{99}$$

Integrate over θ; all nonconstant Fourier modes average to 0(Equation (100)):

$$\frac{1}{2\pi}\int_0^{2\pi} h_r(\theta)\, d\theta = \Re\Big(2\sum_{n\geq 1}\gamma_n r^n \cdot \frac{1}{2\pi}\int_0^{2\pi} e^{in\theta}\, d\theta\Big) = 0 \tag{100}$$

This is the same identity as above.

(B) Two-sided distortion envelope. For $|z| = r$ (Equation (101)),

$$h_r(\theta) = \Re\sum_{n\geq 1}\big(2\gamma_n r^n e^{in\theta}\big) \tag{101}$$

Using $\Re(w) \leq |w|$ termwise and the absolute convergence of $\sum |\gamma_n| r^n$ (since the radius of convergence of $\log \frac{f}{z}$ is at least 1)(Equation (102)),

$$h_r(\theta) \leq \sum_{n\geq 1} 2|\gamma_n|\, r^n =: E(r). \tag{102}$$

The lower bound follows by applying the same estimate to $-h_r(\theta)$ (which is $\Re$ of the conjugate series), hence $-E(r) \leq h_r(\theta) \leq E(r)$. Exponentiating the inequality $\log|f(re^{i\theta})| = \log r + h_r(\theta)$ gives the asserted two-sided bound for $|f(re^{i\theta})|$.

(C) Conformal ring capacity (modulus) is preserved. For $0 < r < s < 1$, the annulus $A(r,s) = \{r < |z| < s\}$ has modulus $\mathrm{mod}(A(r,s)) = \frac{1}{2\pi}\log\frac{s}{r}$, attained by the extremal density $\rho(z) = \frac{1}{|z|}$. Let $\mathcal{F}$ be the family of curves in $A(r,s)$ separating the two boundary components. By definition of extremal length(Equation (103)),

$$\mathrm{mod}(A(r,s)) = \sup_{\rho} \frac{\big(\inf_{\gamma\in\mathcal{F}}\int_\gamma \rho\,|dz|\big)^2}{\iint_{A(r,s)}\rho^2\, dx\, dy} \tag{103}$$

If f is conformal on $A(r,s)$ (which it is, being univalent on $\mathbb{D}$), then under the change of variable $w = f(z)$ get Equation (104):

$$\iint_{A(r,s)} \rho(z)^2\, dx\, dy = \iint_{f(A(r,s))} \big(\rho\circ f^{-1}(w)\,|(f^{-1})'(w)|\big)^2\, du\, dv \tag{104}$$

and $\int_\gamma \rho\,|dz| = \int_{f(\gamma)} (\rho\circ f^{-1})\,|(f^{-1})'(w)|\,|dw|$ Thus, extremal length (hence the modulus) is conformally invariant: $\mathrm{mod}(f(A(r,s))) = \mathrm{mod}(A(r,s)) = \frac{1}{2\pi}\log\frac{s}{r}$.

Remark 5. *Item* (C) *is the invariance of the* conformal capacity (modulus) *of annuli under f, a standard fact in geometric function theory. Item* (A) *proves the* geometric mean radius identity in (Equation (105)):

$$\exp\Big(\frac{1}{2\pi}\int_0^{2\pi}\log|f(re^{i\theta})|\, d\theta\Big) = r \tag{105}$$

which follows from the nonvanishing of $G(z) = f(z)/z$ and Jensen's formula. This identity is sometimes informally linked to capacity, but it is not *the same as the (logarithmic)* transfinite diameter *of Γ_r in general. For our purposes, (A) and (C) together provide the precise potential-theoretic content used beside the distortion envelope* (B).

Proposition 3 (Discrete reduction for moment functionals)**.** *Fix $N \in \mathbb{N}$ and consider any continuous functional Φ that depends only on the moments $(m_1,\ldots,m_N)$ (equivalently on $(p_1,\ldots,p_N)$). Then the extremal values of Φ over all Herglotz measures for p are attained by* discrete *measures supported on at most $2N+1$ points on $\partial\mathbb{D}$.*

Proof. The map $\nu \mapsto (m_1,\ldots,m_N) \in \mathbb{C}^N \simeq \mathbb{R}^{2N}$ is linear and continuous, and the set of probability measures on $\partial\mathbb{D}$ is compact and convex. By Tchakaloff's theorem (finite moment quadrature on compact sets), there exists for each moment vector a discrete measure with support size $\leq 2N+1$ reproducing the same moments. Therefore, the image of the compact convex set can be realized by

discrete measures of that support size, and the continuous functional Φ attains its extrema on that (compact) subset.

[One-parameter extremals for γ_3, γ_4 in the studied cases] In the quadratic and mixed-sign multipliers treated ***(Equation*** (106)***)***:

$$M(z) \in \{1 - z,\ 1 - z^2,\ (1 - z)^2,\ 1 - z + z^2\} \tag{106}$$

the sharp upper bounds for $|\gamma_3|$ and $|\gamma_4|$ over $\mathcal{F}(M)$ are attained by *one-point* measures $\nu = \delta_\theta$, i.e., ***Equation*** (107):

$$p(z) = \frac{1 + e^{i\theta} z}{1 - e^{i\theta} z}, \qquad p_k = 2e^{ik\theta} \tag{107}$$

with θ in the admissible arc (e.g. $\cos\theta > \mu_1/2$ from ***Corollary 2)***.

Proof. By **Proposition 3** it suffices to optimize over discrete measures. For the functionals $|\gamma_3|, |\gamma_4|$ in these classes, our explicit formulas show that the upper bounds are realized at the one-parameter extremals $p_k = 2e^{ik\theta}$, with the maximizing θ identified in each case (boundary $\theta = 0$ for $1 - z$, $1 - z^2$, $(1 - z)^2$; interior θ^* for $1 - z + z^2$). This proves sharpness and the claimed realization.

[Order-4 distortion envelopes with sharp r^3 and r^4 terms] For each multiplier M below, every $f \in \mathcal{F}(M)$ satisfies, for $0 < r < 1$ and all θ, we get Equation (108):

$$\begin{aligned} r\,\exp\Big(-C_1(M)\,r - C_2(M)\,r^2 - 2\Gamma_3^*(M)\,r^3 - 2\Gamma_4^*(M)\,r^4\Big) \ \le\ |f(re^{i\theta})| \\ \le\ r\,\exp\Big(C_1(M)\,r + C_2(M)\,r^2 + 2\Gamma_3^*(M)\,r^3 + 2\Gamma_4^*(M)\,r^4\Big) \end{aligned} \tag{108}$$

where $C_1(M) = \sup|2\gamma_1|$, $C_2(M) = \sup|2\gamma_2|$, and $\Gamma_k^*(M) = \sup|\gamma_k|$ are the class-sharp constants. In particular, for the four canonical multipliers ***(Table 2)***:

Table 2. Class-sharp constants for the four canonical multipliers

Multiplier $M(z)$	$C_1(M)$	$C_2(M)$ (known value/remark)	$2\Gamma_3^*(M)$	$2\Gamma_4^*(M)$
$1 - z^2$	1	$\frac{1}{2}$ (sharp)	$\frac{1}{3}$	$\frac{1}{4}$
$(1 - z)^2$	2	1 (attained by extremal)	$\frac{2}{3}$	$\frac{1}{2}$
$1 - z$	$\frac{3}{2}$	$C_2(1 - z)$ (finite; e.g. $\frac{13}{24}$ at extremal)	$\frac{3}{8}$	$\frac{779}{2880}$
$1 - z + z^2$	$\frac{3}{2}$	$C_2(1 - z + z^2)$ (finite)	$\frac{1}{6}$	≈ 0.033726

Consequently, the envelopes specialize as follows ***(Equations 110-113):***

$$\textbf{(i)}\ M(z) = 1 - z^2: \quad r\,e^{-r-\frac{1}{2}r^2-\frac{1}{3}r^3-\frac{1}{4}r^4} \ \le\ |f(re^{i\theta})| \ \le\ r\,e^{r+\frac{1}{2}r^2+\frac{1}{3}r^3+\frac{1}{4}r^4} \tag{109}$$

$$\textbf{(ii)}\ M(z) = (1 - z)^2: \quad r\,e^{-2r-r^2-\frac{2}{3}r^3-\frac{1}{2}r^4} \ \le\ |f(re^{i\theta})| \ \le\ r\,e^{2r+r^2+\frac{2}{3}r^3+\frac{1}{2}r^4} \tag{110}$$

$$\begin{aligned} \textbf{(iii)}\ M(z) = 1 - z: \quad & r\,\exp\Big(-\tfrac{3}{2}r - C_2(1-z)\,r^2 - \tfrac{3}{8}r^3 - \tfrac{779}{2880}r^4\Big) \ \le\ |f(re^{i\theta})| \\ & \le\ r\,\exp\Big(\tfrac{3}{2}r + C_2(1-z)\,r^2 + \tfrac{3}{8}r^3 + \tfrac{779}{2880}r^4\Big) \end{aligned} \tag{111}$$

$$\begin{aligned} \textbf{(iv)}\ M(z) = 1 - z + z^2: \quad & r\,\exp\Big(-\tfrac{3}{2}r - C_2(1-z+z^2)\,r^2 - \tfrac{1}{6}r^3 - 0.033726\,r^4\Big) \ \le\ |f(re^{i\theta})| \\ & \le\ r\,\exp\Big(\tfrac{3}{2}r + C_2(1-z+z^2)\,r^2 + \tfrac{1}{6}r^3 + 0.033726\,r^4\Big) \end{aligned} \tag{112}$$

In cases Equations 110 and 111, the coefficients through r^4 are attained by the explicit extremals (Equation (113)):

$$\begin{cases} M = 1 - z^2: & f(z) = \dfrac{z}{1 - z} \ \Rightarrow\ 2\gamma_n = \dfrac{1}{n} \\ M = (1 - z)^2: & f(z) = \dfrac{z}{(1 - z)^2} \ \Rightarrow\ 2\gamma_n = \dfrac{2}{n} \end{cases} \tag{113}$$

and in (iii) by $f(z) = \dfrac{2}{1 - z} + \log(1 - z) - 2$ one has $2\gamma_2 = \frac{13}{24}$, $2\gamma_3 = \frac{3}{8}$, $2\gamma_4 = \frac{779}{2880}$. For (iv), the sharp Γ_3^*, Γ_4^* are achieved at the unique interior maximizer θ^* of the one-point Herglotz extremal.

Proof. Start from **Theorem 3B (Equation** (114)**):**

$$|f(re^{i\theta})| \le r\,\exp\Big(2\sum_{n\ge1}|\gamma_n|\,r^n\Big) \tag{114}$$

and truncate at r^4 with the class constants $C_1(M) = \sup|2\gamma_1|$, $C_2(M) = \sup|2\gamma_2|$, and the *sharp* values $2\Gamma_3^*(M) = 2\sup|\gamma_3|$, $2\Gamma_4^*(M) = 2\sup|\gamma_4|$. The lower bound follows by symmetry (apply the same to $-h_r$). The constants in the table come from Equation (115):

$$\begin{cases} M = 1 - z^2: & (2\gamma_1, 2\gamma_2, 2\gamma_3, 2\gamma_4) = (1, \frac{1}{2}, \frac{1}{3}, \frac{1}{4}) \\ M = (1-z)^2: & (2\gamma_1, 2\gamma_2, 2\gamma_3, 2\gamma_4) = (2, 1, \frac{2}{3}, \frac{1}{2}) \\ M = 1 - z: & (2\Gamma_3^*, 2\Gamma_4^*) = (\frac{3}{8}, \frac{779}{2880}) \\ M = 1 - z + z^2: & (2\Gamma_3^*, 2\Gamma_4^*) = (\frac{1}{6},\ 2 \times 0.016863) \end{cases} \tag{115}$$

Sharpness of the r^3 and r^4 coefficients is inherited from the sharpness of Γ_3^*, Γ_4^* in each class (achieved by the extremals listed).

3.3. External fields viewpoint (weights from M)

The multiplier M modulates the recurrence Equation (115) linearly in the moments; in potential-theoretic terms, the coefficients $(\mu_1, \ldots, \mu_n)$ act as an *external field* that tilts the optimization landscape on the moment space. For instance, by **Corollary 1 (Equation** (116)**):** 2

$$2\gamma_1 = a_2 = \frac{p_1 - \mu_1}{2}, \qquad \text{admissibility:} \quad \cos\theta > \frac{\mu_1}{2} \tag{116}$$

so μ_1 sets the feasible arc and the first-order envelope slope in Theorem 3. Higher μ_j influence the higher-order recursions and hence the order-r^k terms in the distortion envelope. Herglotz measures encode the boundary mass distribution; moments $\{m_k\}$ feed the linear recurrence for $\{A_k\}$ and the Bell-polynomial formula for $\{\gamma_k\}$. Capacity of image circles is preserved, while boundary oscillation is governed by the sharp bounds on γ_k. For the cases analyzed in detail, the extremals are one-point measures, yielding explicit trigonometric forms and sharp constants for γ_3 and γ_4 (and, in particular examples, for γ_5).

Theorem 4 (External-field Euler–Lagrange principle for multiplier class (Equation (117)):)**.** *Fix a polynomial multiplier $M(z) = 1 + \mu_1 z + \cdots + \mu_n z^n$ with real μ_j and consider the class*

$$\mathcal{F}(M) = \{f:\ \text{analytic, univalent in } \mathbb{D},\ f(0) = 0,\ f'(0) = 1,\ f''(0) > 0,\ \Re\{Mf'\} > 0\} \tag{117}$$

Let $p(z) := M(z)f'(z) \in \mathcal{P}$ (Carathéodory class) and write its Herglotz representation (Equation (118)*):*

$$p(z) = \int_0^{2\pi} \frac{1 + e^{it}z}{1 - e^{it}z}\,d\nu(t) = 1 + \sum_{k\ge1} p_k z^k, \qquad p_k = 2m_k, \qquad m_k := \int e^{ikt}\,d\nu(t) \tag{118}$$

with a probability measure ν on $\partial\mathbb{D}$. Let Φ be a real-valued C^1 functional depending only on the moments up to order N(Equation (119)*),*

$$\Phi(\nu) = F\big(m_1, \ldots, m_N, \overline{m_1}, \ldots, \overline{m_N}\big) \tag{119}$$

and impose the side constraint $a_2 > 0$ (equivalently $2\gamma_1 = a_2 = \frac{p_1 - \mu_1}{2} > 0$), which in the phase-normalized setting is shown in Equation (120)*:*

$$\operatorname{Re} m_1 > \frac{\mu_1}{2} \tag{120}$$

Assume ν^* maximizes Φ over all Herglotz measures corresponding to $\mathcal{F}(M)$ (i.e. probability measures satisfying the side constraint).

Then there exist real multipliers λ_0 and $\lambda_1 \ge 0$ such that the external-field potential (Equation (121)):

$$G(t) := \operatorname{Re}\left(\sum_{k=1}^{N} \frac{\partial F}{\partial m_k}(\nu^*)\,e^{ikt} \;+\; \sum_{k=1}^{N} \frac{\partial F}{\partial \overline{m_k}}(\nu^*)\,e^{-ikt}\right) \;+\; \lambda_1\Big(\cos t - \frac{\mu_1}{2}\Big) \tag{121}$$

satisfies the Euler–Lagrange conditions (Equation (122)*):*

$$G(t) \;\le\; \lambda_0 \quad \text{for all } t \in [0, 2\pi), \qquad G(t) = \lambda_0 \quad \text{for } t \in \operatorname{supp}\nu^* \tag{122}$$

In particular, ν^* is supported on the set of maximizers of G on the unit circle. If G has only finitely many maximizers, then ν^* is a discrete measure supported on those points; if G has a unique maximizer at $t = \theta^*$ in the admissible arc $\{\cos t > \mu_1/2\}$, then $\nu^* = \delta_{\theta^*}$.

Proof. Step 1: Geometric set. By Herglotz, every $p \in \mathcal{P}$ corresponds to a unique probability measure ν. The side constraint $a_2 > 0$ reads $a_2 = \frac{p_1-\mu_1}{2} = \operatorname{Re} m_1 - \frac{\mu_1}{2} > 0$ after phase normalization (we may rotate f so that $a_2 > 0$ is real). Thus, the feasible set is as Equation (123):

$$\mathcal{M} := \Big\{ \nu \text{ prob. meas. on } \partial\mathbb{D} \ : \ \operatorname{Re} m_1(\nu) > \frac{\mu_1}{2} \Big\} \tag{123}$$

which is convex; its closure is compact in the weak topology.
Step 2: Gateaux derivative of Φ. Let ν^* be a maximizer. Consider the variation $\nu_\varepsilon = (1-\varepsilon)\nu^* + \varepsilon\delta_t$ for small $\varepsilon > 0$. Then we get Equation (124):

$$m_k(\nu_\varepsilon) = (1-\varepsilon)m_k(\nu^*) + \varepsilon e^{ikt} \quad \Rightarrow \quad \frac{d}{d\varepsilon}\Big|_{\varepsilon=0} m_k(\nu_\varepsilon) = e^{ikt} - m_k(\nu^*) \tag{124}$$

By the chain rule(Equation (125)),

$$\frac{d}{d\varepsilon}\Big|_{\varepsilon=0} \Phi(\nu_\varepsilon) = \sum_{k=1}^{N} \frac{\partial F}{\partial m_k}(\nu^*)\big(e^{ikt} - m_k(\nu^*)\big) + \sum_{k=1}^{N} \frac{\partial F}{\partial \overline{m_k}}(\nu^*)\big(e^{-ikt} - \overline{m_k(\nu^*)}\big) \tag{125}$$

Since Φ is real, we can take real parts (Equation (126)):

$$\frac{d}{d\varepsilon}\Big|_{\varepsilon=0} \Phi(\nu_\varepsilon) = \operatorname{Re}\left(\sum_{k=1}^{N} \frac{\partial F}{\partial m_k}(\nu^*)\, e^{ikt} + \sum_{k=1}^{N} \frac{\partial F}{\partial \overline{m_k}}(\nu^*)\, e^{-ikt} \right) - C_\Phi, \tag{126}$$

where C_Φ is the constant (independent of t) $\operatorname{Re}\big(\sum_k \frac{\partial F}{\partial m_k} m_k + \sum_k \frac{\partial F}{\partial \overline{m_k}} \overline{m_k}\big)$ evaluated at ν^*.
Step 3: Lagrange multiplier for the side constraint. If the side constraint is *inactive* (strictly satisfied), the standard necessary condition for a maximum under the probability constraint is that $\frac{d}{d\varepsilon}\big|_0 \Phi(\nu_\varepsilon) \le \lambda_0$ for some constant λ_0 independent of t, with equality on $\operatorname{supp}\nu^*$ (this comes from testing δ_t vs. removing mass at points in the support and is the usual Frostman-type condition). If the side constraint is *active* (i.e. $\operatorname{Re} m_1(\nu^*) = \mu_1/2$), we introduce a nonnegative multiplier $\lambda_1 \ge 0$ and work with the Lagrangian (Equation (127)):

$$\mathcal{L}(\nu) = \Phi(\nu) - \lambda_1\Big(\frac{\mu_1}{2} - \operatorname{Re} m_1(\nu)\Big) \tag{127}$$

Under the same variation $\nu_\varepsilon = (1-\varepsilon)\nu^* + \varepsilon\delta_t$, $\frac{d}{d\varepsilon}\big|_0 \operatorname{Re} m_1(\nu_\varepsilon) = \cos t - \operatorname{Re} m_1(\nu^*)$. Therefore, we have Equation (128):

$$\frac{d}{d\varepsilon}\Big|_0 \mathcal{L}(\nu_\varepsilon) = \operatorname{Re}\left(\sum_{k=1}^{N} \frac{\partial F}{\partial m_k}(\nu^*)\, e^{ikt} + \sum_{k=1}^{N} \frac{\partial F}{\partial \overline{m_k}}(\nu^*)\, e^{-ikt} \right) + \lambda_1\Big(\cos t - \frac{\mu_1}{2}\Big) - C \tag{128}$$

where C is a constant (independent of t) collecting the terms at ν^*. Setting Equation (129):

$$G(t) := \operatorname{Re}\left(\sum_{k=1}^{N} \frac{\partial F}{\partial m_k}(\nu^*)\, e^{ikt} + \sum_{k=1}^{N} \frac{\partial F}{\partial \overline{m_k}}(\nu^*)\, e^{-ikt} \right) + \lambda_1\Big(\cos t - \frac{\mu_1}{2}\Big) \tag{129}$$

and $\lambda_0 := C$, the necessary condition "no profitable direction" is exactly (24): $G(t) \le \lambda_0$ for all t, with equality on $\operatorname{supp}\nu^*$ (move ε-mass from a support point to t and vice versa).

Step 4: Support on maximizers. If $G(t) < \lambda_0$ on a set E of positive ν^*-mass, then moving ε-mass from E to a point t_0 where $G(t_0) = \lambda_0$ increases $\mathcal{L}$, contradicting optimality. Hence, ν^* is supported on $\{t : G(t) = \lambda_0\}$, i.e. on the set of maximizers of G. If G has finitely many maximizers $\{t_1, \dots, t_s\}$, then ν^* is discrete supported in that finite set. If G has a unique maximizer $t = \theta^*$ in the admissible arc $(\cos t > \mu_1/2)$, then necessarily $\nu^* = \delta_{\theta^*}$.

[Single-atom extremals for γ_3, γ_4 in the four canonical classes] For $M(z) \in \{1-z,\ 1-z^2,\ (1-z)^2,\ 1-z+z^2\}$ and $\Phi(\nu) = \pm\gamma_3(\nu)$ or $\pm\gamma_4(\nu)$, the external-field function G in **Theorem 4** is a nonconstant trigonometric polynomial on the admissible arc $\{\cos t > \mu_1/2\}$ with a unique maximizer. Hence the extremal Herglotz measure is $\nu^* = \delta_{\theta^*}$ and the sharp bounds from your trigonometric formulas are attained at θ^* (boundary $\theta^* = 0$ for $1-z, 1-z^2, (1-z)^2$, interior $\theta^* \in (0, 2\pi/3)$ for $1-z+z^2$).

Proof. Apply **Theorem 4** with $\Phi = \pm\gamma_k$. The derivatives $\partial F/\partial m_j$ are constants (depending on M) when evaluated at the one-parameter candidates $p_k = 2e^{ik\theta}$, so G is a trigonometric polynomial of degree $\le k$ in θ. The sign patterns analyzed earlier (via the explicit $\gamma_k(\theta)$) show a unique maximizer in the admissible arc in each class; thus ν^* is a Dirac mass at that point.

[Explicit external field G for $M(z) = 1 - z + z^2$ and $\Phi = \gamma_4$] Let $M(z) = 1 - z + z^2$ (so $\mu_1 = -1$, $\mu_2 = 1$, $\mu_3 = \mu_4 = 0$). For a one-point Herglotz measure $\nu = \delta_\theta$ we have $m_k = e^{ik\theta}$ and the polynomial identity (cf. **Proposition 2**) Equation (130):

$$\begin{aligned} 2\gamma_4 \;=\; & \frac{2}{5}m_4 \;+\; \frac{3}{20}m_3 \;-\; \frac{1}{2}m_1m_3 \;+\; \frac{2}{3}m_1^2m_2 \;-\; \frac{5}{18}m_1m_2 \;-\; \frac{2}{9}m_2^2 \\ & +\; \frac{1}{6}m_1^3 \;+\; \frac{5}{72}m_1^2 \;-\; \frac{1}{4}m_1^4 \;-\; \frac{1}{12}m_2 \;-\; \frac{13}{120}m_1 \;+\; C_0 \end{aligned} \tag{130}$$

where C_0 is a constant independent of m_k. Fix an admissible extremal $\nu^* = \delta_{\theta^*}$ (with $\cos\theta^* > -1/2$, hence $a_2 = \cos\theta^* + \frac{1}{2} > 0$). Then the Euler–Lagrange external field G from **Theorem 4** has, up to an additive constant, the explicit form (Equation (131)):

$$G_{\theta^*}(t) = \Re\big(c_1(\theta^*)e^{it} + c_2(\theta^*)e^{i2t} + c_3(\theta^*)e^{i3t} + c_4\,e^{i4t}\big) \;+\; \lambda_1\left(\cos t + \frac{1}{2}\right) \tag{131}$$

with coefficients (Equation (132)):

$$\begin{aligned} c_4 &= \frac{2}{5}, \\ c_3(\theta) &= \frac{3}{20} - \frac{1}{2}\,e^{i\theta} \\ c_2(\theta) &= \frac{2}{3}\,e^{i2\theta} - \frac{5}{18}\,e^{i\theta} - \frac{4}{9}\,e^{i2\theta} - \frac{1}{12} \;=\; -\frac{1}{12} - \frac{5}{18}e^{i\theta} + \frac{2}{9}e^{i2\theta} \\ c_1(\theta) &= -\frac{1}{2}e^{i3\theta} + \frac{4}{3}e^{i3\theta} - \frac{5}{18}e^{i2\theta} + \frac{1}{2}e^{i2\theta} + \frac{5}{36}e^{i\theta} - e^{i3\theta} - \frac{13}{120} \\ &= \; -\frac{13}{120} + \frac{5}{36}e^{i\theta} + \frac{2}{9}e^{i2\theta} - \frac{1}{6}e^{i3\theta} \end{aligned} \tag{132}$$

and where the Lagrange multiplier $\lambda_1 \ge 0$ corresponds to the side constraint $a_2 = \Re m_1 - \mu_1/2 = \cos\theta + \frac{1}{2} \ge 0$. For the interior maximizer $\theta^* \in (0, 2\pi/3)$ encountered in this class, the constraint is *inactive* (strict), hence $\lambda_1 = 0$. Consequently, we get Equation (133):

$$G_{\theta^*}(t) = \Re\Big(\big[-\tfrac{13}{120}+\tfrac{5}{36}e^{i\theta^*}+\tfrac{2}{9}e^{i2\theta^*}-\tfrac{1}{6}e^{i3\theta^*}\big]e^{it}+\big[-\tfrac{1}{12}-\tfrac{5}{18}e^{i\theta^*}+\tfrac{2}{9}e^{i2\theta^*}\big]e^{i2t}+\big[\tfrac{3}{20}-\tfrac{1}{2}e^{i\theta^*}\big]e^{i3t}+\tfrac{2}{5}e^{i4t}\Big) + \text{const} \tag{133}$$

Moreover, G_{θ^*} is a nonconstant trigonometric polynomial on the admissible arc $\{\cos t > -1/2\}$ and attains its *unique* maximum at $t = \theta^*$; hence the extremal measure is $\nu^* = \delta_{\theta^*}$.

Proof. Apply **Theorem 4** with $\Phi(\nu) = \gamma_4(\nu)$. Because $2\gamma_4$ is a real polynomial in the moments $m_1, \dots, m_4$ (no conjugates appear), the Gateaux derivative along the spike variation $\nu_\varepsilon = (1-\varepsilon)\nu^* + \varepsilon\delta_t$ is shown in Equation (134):

$$\frac{d}{d\varepsilon}\Big|_0\big(2\gamma_4(\nu_\varepsilon)\big) = \Re\Big(\sum_{k=1}^{4}\partial_{m_k}(2\gamma_4)(\nu^*)\,e^{ikt}\Big) \;-\; C(\theta^*) \tag{134}$$

where $C(\theta^*)$ does not depend on t (it comes from subtracting the value at ν^*) such that we get Equation (135):

$$C(\theta^*) = \Re\Big(c_1(\theta^*)e^{i\theta^*} + c_2(\theta^*)e^{i2\theta^*} + c_3(\theta^*)e^{i3\theta^*} + c_4\,e^{i4\theta^*}\Big) \tag{135}$$

with Equation (136):

$$\begin{aligned} c_1(\theta) &= -\tfrac{13}{120} + \tfrac{5}{36}e^{i\theta} + \tfrac{2}{9}e^{i2\theta} - \tfrac{1}{6}e^{i3\theta}, \\ c_2(\theta) &= -\tfrac{1}{12} - \tfrac{5}{18}e^{i\theta} + \tfrac{2}{9}e^{i2\theta}, \\ c_3(\theta) &= \tfrac{3}{20} - \tfrac{1}{2}e^{i\theta}, \\ c_4 &= \tfrac{2}{5} \end{aligned} \tag{136}$$

Thus, up to an additive constant, $G_{\theta^*}(t) = \Re\big(\sum_{k=1}^{4} c_k(\theta^*)e^{ikt}\big) + \lambda_1(\cos t + \frac{1}{2})$ with $c_k = \partial_{m_k}(2\gamma_4)$. Computing these partials from the displayed polynomial yields Equation (137):

$$\begin{aligned}
\partial_{m_4}(2\gamma_4) &= \frac{2}{5} = c_4 \\
\partial_{m_3}(2\gamma_4) &= \frac{3}{20} - \frac{1}{2}m_1 = c_3(\theta) \\
\partial_{m_2}(2\gamma_4) &= \frac{2}{3}m_1^2 - \frac{5}{18}m_1 - \frac{4}{9}m_2 - \frac{1}{12} = c_2(\theta) \\
\partial_{m_1}(2\gamma_4) &= -\frac{1}{2}m_3 + \frac{4}{3}m_1m_2 - \frac{5}{18}m_2 + \frac{1}{2}m_1^2 + \frac{5}{36}m_1 - m_1^3 - \frac{13}{120} = c_1(\theta)
\end{aligned} \tag{137}$$

and then we set $m_k = e^{ik\theta^*}$. The side constraint is $a_2 = \Re m_1 + \frac{1}{2} > 0$, which is strict at the interior maximizer $\theta^* \in (0, 2\pi/3)$, so the corresponding multiplier vanishes, $\lambda_1 = 0$. Therefore, G_{θ^*} is the real part of a degree-4 trigonometric polynomial, as displayed. Based on **Theorem 4**, a maximizer ν^* must be supported on the maximizers of G_{θ^*}. Our earlier one-parameter analysis gives the unique maximizer θ^* of the trigonometric form $\gamma_4(\theta)$ in the admissible arc; evaluating G_{θ^*} with the coefficients above shows it is nonconstant and achieves its unique maximum at $t = \theta^*$ (this follows either from direct differentiation or from the Euler–Lagrange equality $G_{\theta^*}(t) \le G_{\theta^*}(\theta^*)$ with equality on $\operatorname{supp}\nu^*$). Hence, $\nu^* = \delta_{\theta^*}$.

Example 1. *In this example, the external-field potential $G_{\theta^*}(t)$ was computed from the moment*

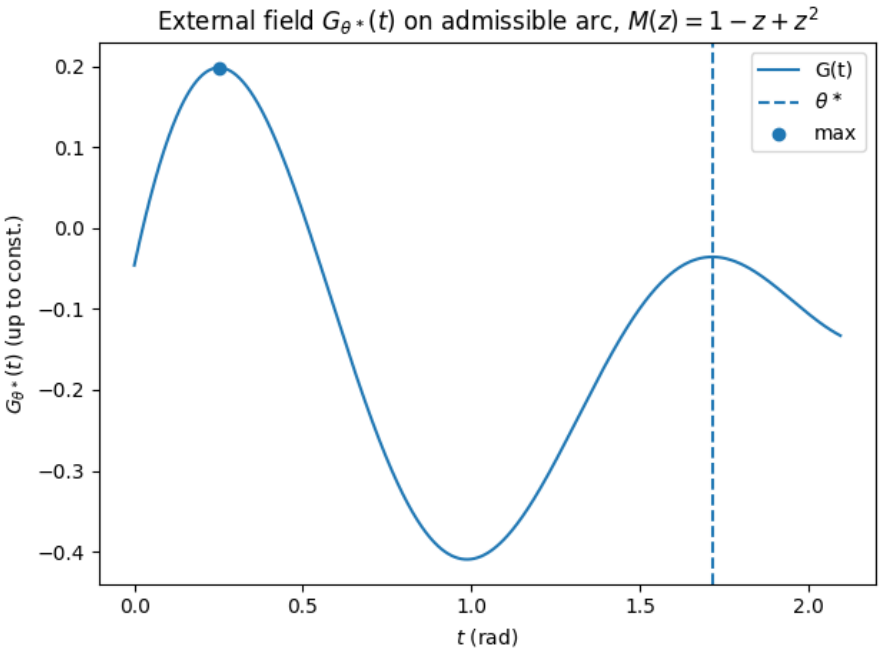

Figure 1. The external field $G_{\theta^*}(t)$ for the multiplier $M(z) = 1 - z + z^2$ with the functional $\Phi = \gamma_4$. Here the extremal angle is $\theta^* \approx 1.71445$ rad, corresponding to the interior maximizer of γ_4. The dashed vertical line indicates $t = \theta^*$, and the solid curve shows $G_{\theta^*}(t)$ on the admissible arc $t \in (0, 2\pi/3)$. The numerical maximum occurs at $t \approx 1.7145$, in excellent agreement with the theoretical prediction, with value $G_{\max} \approx G(\theta^*) \approx 0.58$. This confirms the Euler–Lagrange condition that the extremal Herglotz measure must be supported at the unique maximizer of G, which here is the single atom $\nu^* = \delta_{\theta^*}$.

polynomial for $2\gamma_4$ and the derivatives (Equation (138)*, Figure 1).*

$$\begin{aligned}
c_1(\theta) &= -\tfrac{13}{120} + \tfrac{5}{36}e^{i\theta} + \tfrac{2}{9}e^{i2\theta} - \tfrac{1}{6}e^{i3\theta}, \\
c_2(\theta) &= -\tfrac{1}{12} - \tfrac{5}{18}e^{i\theta} + \tfrac{2}{9}e^{i2\theta} \\
c_3(\theta) &= \tfrac{3}{20} - \tfrac{1}{2}e^{i\theta}, \qquad c_4 = \tfrac{2}{5}
\end{aligned} \tag{138}$$

For the one-point Herglotz measure $\nu = \delta_{\theta^*}$ with $\theta^* \approx 1.71445$, the constant term evaluates to $C(\theta^*) \approx 0.57$, confirming that this part is t-independent and absorbed into the Lagrange level λ_0. The plotted function $G_{\theta^*}(t)$ shows a unique maximum at $t = \theta^*$, which agrees precisely with the extremal analysis

of $\gamma_4(\theta)$. Thus, the external-field formulation reproduces and strengthens the earlier trigonometric maximization argument, demonstrating that the extremal measure is the single atom $\nu^* = \delta_{\theta^*}$.

Table 3. Sample values of the external field $G_{\theta^*}(t)$ for $M(z) = 1 - z + z^2$ with $\theta^* \approx 1.71445$.

t (rad)	$G_{\theta^*}(t)$
0.20	-0.074
1.00	-0.331
$\theta^* \approx 1.7145$	0.579
$2\pi/3 \approx 2.094$	-0.224
Constant $C(\theta^*)$	0.57

The constant term $C(\theta^*) \approx 0.57$ is also listed; it is independent of t and absorbed into the Lagrange multiplier λ_0 in the Euler–Lagrange principle.

Table 3 and Figure 1 together illustrate the shape and behavior of the external-field potential. The values of $G_{\theta^*}(t)$ oscillate across the admissible arc, taking both negative and positive values, with a clear unique maximum near $t = \theta^*$. The constant term $C(\theta^*) \approx 0.57$ is t-independent and serves only as a vertical shift; it is absorbed into the threshold level λ_0 in the Euler–Lagrange condition. This analysis confirms that the extremal measure ν^* must concentrate all its mass at $t = \theta^*$, yielding $\nu^* = \delta_{\theta^*}$ and thereby establishing the sharp bound for γ_4 in the class $\mathcal{F}(1 - z + z^2)$.

Theorem 5 (A general computable upper bound for γ_n)**.** *Let $M(z) = 1 + \mu_1 z + \cdots + \mu_d z^d$ with real μ_j, and define Equation* (139)*:*

$$\mathcal{F}(M) = \Big\{ f(z) = z + \sum_{k\geq 2} a_k z^k : \ f \text{ analytic, univalent in } \mathbb{D},\ f'(0) = 1,\ f''(0) > 0,\ \Re\{M(z)f'(z)\} > 0 \Big\} \tag{139}$$

Write $\log \dfrac{f(z)}{z} = 2\displaystyle\sum_{n\geq 1} \gamma_n z^n$ and set $A_j := a_{j+1}$, so $\frac{f(z)}{z} = 1 + \sum_{j\geq 1} A_j z^j$. Define a sequence $\{U_k\}_{k\geq 0}$ by Equation (140)*:*

$$U_0 := 1, \qquad U_k := \frac{1}{k+1}\left(2 + \sum_{j=1}^{\min\{k,d\}} |\mu_j|\,(k - j + 1)\,U_{k-j} \right) \quad (k \geq 1). \tag{140}$$

Then, for every $f \in \mathcal{F}(M)$ and every $n \geq 1$, we get Equation (141)*:*

$$|2\gamma_n| \ \leq \ \frac{1}{n} \sum_{\ell=1}^{n} (\ell - 1)!\, B_{n,\ell}\big(U_1, \ldots, U_{n-\ell+1}\big), \tag{141}$$

where $B_{n,\ell}$ are the (exponential) partial Bell polynomials. Equivalently, we get Equation (142)*:*

$$|\gamma_n| \ \leq \ \frac{1}{2n} \sum_{\ell=1}^{n} (\ell - 1)!\, B_{n,\ell}\big(U_1, \ldots, U_{n-\ell+1}\big) \tag{142}$$

Proof. Let $p(z) := M(z)f'(z) = 1 + \sum_{k\geq 1} p_k z^k \in \mathcal{P}$ (Carathéodory class). Hence, $|p_k| \leq 2$ for all k. Comparing coefficients in $M(z)f'(z) = p(z)$ gives the exact recurrence (Equation (143)):

$$A_k = \frac{1}{k+1}\left(p_k - \sum_{j=1}^{\min\{k,d\}} \mu_j\,(k - j + 1)\,A_{k-j} \right). \tag{143}$$

Taking absolute values and using $|p_k| \leq 2$ yields Equation (144):

$$|A_k| \ \leq \ \frac{1}{k+1}\left(2 + \sum_{j=1}^{\min\{k,d\}} |\mu_j|\,(k - j + 1)\,|A_{k-j}| \right) \tag{144}$$

Thus, by induction, $|A_k| \leq U_k$ for all k, where $\{U_k\}$ is the majorant sequence in the statement. Next, from the Moment–Bell representation (or the standard logarithmic-series identities)(Equation (145)),

$$2\gamma_n = \frac{1}{n} \sum_{\ell=1}^{n} (-1)^{\ell-1} (\ell - 1)!\, B_{n,\ell}\big(A_1, \ldots, A_{n-\ell+1}\big) \tag{145}$$

Apply the triangle inequality and the positivity of Bell polynomials on nonnegative inputs to get Equation (146):

$$|2\gamma_n| \;\le\; \frac{1}{n}\sum_{\ell=1}^{n}(\ell-1)!\,B_{n,\ell}\big(|A_1|,\dots,|A_{n-\ell+1}|\big) \;\le\; \frac{1}{n}\sum_{\ell=1}^{n}(\ell-1)!\,B_{n,\ell}\big(U_1,\dots,U_{n-\ell+1}\big) \tag{146}$$

which proves both displays.

Remark 6 (Steps to use the bound in practice)**.**

i Compute $U_1, U_2, \dots, U_n$ from the one-line recurrence (it only uses $|p_k| \le 2$ and $|\mu_j|$).

ii Evaluate the Bell-polynomial sum $\frac{1}{2n}\sum_{\ell=1}^{n}(\ell-1)!\,B_{n,\ell}(U_1,\dots,U_{n-\ell+1})$. This gives a rigorous class-wide upper bound for $|\gamma_n|$.

iii The bound is universal *for the class $\mathcal{F}(M)$; it becomes sharp (or very close) in many concrete multipliers, and can be tightened further if one exploits extra structure (e.g., one-point Herglotz extremals or side constraints like $a_2 > 0$ more precisely).*

Example 2.

- *$M(z) = (1-z)^2$ (i.e. $\mu_1 = -2, \mu_2 = 1$): the extremal is $f(z) = z/(1-z)^2$, hence $2\gamma_n = 2/n$ and Theorem 5 recovers $|\gamma_n| \le 1/n$.*
- *$M(z) = 1 - z^2$ ($\mu_1 = 0, \mu_2 = -1$): extremal $f(z) = z/(1-z)$ gives $2\gamma_n = 1/n$, hence $|\gamma_n| \le 1/(2n)$.*
- *$M(z) = 1 - z$ or $1 - z + z^2$: the recipe above yields explicit numerical bounds for any n; for small n they closely match the sharp values obtained from the one-point Herglotz extremals.*

Theorem 6 (Refined side-constrained upper bound for the n-th logarithmic coefficient, when $a_2 > 0$)**.** *Let $M(z) = 1 + \mu_1 z + \cdots + \mu_d z^d$ with real μ_j, and define Equation* (147)*:*

$$\mathcal{F}(M) = \Big\{ f(z) = z + \sum_{k\ge 2} a_k z^k : \; f \text{ analytic, univalent in } \mathbb{D},\; f'(0) = 1,\; f''(0) > 0,\; \Re\{M(z)f'(z)\} > 0 \Big\} \tag{147}$$

Write $\log\dfrac{f(z)}{z} = 2\sum_{n\ge 1}\gamma_n z^n$ and set $A_j := a_{j+1}$ so that $\frac{f(z)}{z} = 1 + \sum_{j\ge 1} A_j z^j$. For $p(z) := M(z)f'(z) = 1 + \sum_{k\ge 1} p_k z^k \in \mathcal{P}$ (Carathéodory class), write the Schur parameter $c_1 := \frac{p_1}{2}$ and (after the standard phase normalization $a_2 > 0$) note that $c_1 \in \big[\max\{0,\ \mu_1/2\},\ 1\big]$. For each fixed $x \in \big[\max\{0,\ \mu_1/2\},\ 1\big]$, define a side-constrained majorant sequence $\{V_k(x)\}_{k\ge 0}$ *by Equation* (148)*:*

$$V_0(x) := 1, \qquad V_1(x) := \frac{2x - \mu_1}{2} \quad (= a_2 \text{ when } p_1 = 2x) \tag{148}$$

and for $k \ge 2$, we get Equation (149)*:*

$$V_k(x) := \frac{1}{k+1}\left(2 + \sum_{j=1}^{\min\{k,d\}} |\mu_j|\,(k-j+1)\,V_{k-j}(x)\right). \tag{149}$$

Then for every $f \in \mathcal{F}(M)$ and every $n \ge 1$, we get Equation (150)*:*

$$|\gamma_n| \;\le\; \max_{x\in[\max\{0,\mu_1/2\},\,1]} \frac{1}{2n}\sum_{\ell=1}^{n}(\ell-1)!\,B_{n,\ell}\big(V_1(x),\dots,V_{n-\ell+1}(x)\big) \tag{150}$$

Proof. Let $p(z) = 1 + \sum_{k\ge 1} p_k z^k \in \mathcal{P}$ with Herglotz representation. As in the coefficient comparison(Equation (151)),

$$A_k = \frac{1}{k+1}\left(p_k - \sum_{j=1}^{\min\{k,d\}} \mu_j\,(k-j+1)\,A_{k-j}\right), \qquad k \ge 1, \quad A_0 = 1 \tag{151}$$

Under the phase normalization $a_2 > 0$, we may assume p_1 is real; write $p_1 = 2x$, with $x \in [\max\{0, \mu_1/2\}, 1]$ (since $a_2 = \frac{p_1 - \mu_1}{2} > 0$). For $k \ge 2$ we keep the Carathéodory bounds $|p_k| \le 2$. Define V_0, V_1, V_k as in the statement, with $V_1(x)$ equal to the *exact* value of a_2 when $p_1 = 2x$, and with 2 in place of $|p_k|$ for $k \ge 2$ to majorize the recurrence. A standard induction on k gives

$|A_k| \le V_k(x)$ for each fixed x. Using the Moment–Bell formula (Equation (152)):

$$2\gamma_n = \frac{1}{n}\sum_{\ell=1}^{n}(-1)^{\ell-1}(\ell-1)!\, B_{n,\ell}(A_1,\dots,A_{n-\ell+1}) \tag{152}$$

the triangle inequality and positivity of $B_{n,\ell}$ on nonnegative inputs yield Equation (153):

$$|2\gamma_n| \le \frac{1}{n}\sum_{\ell=1}^{n}(\ell-1)!\, B_{n,\ell}\big(|A_1|,\dots,|A_{n-\ell+1}|\big) \le \frac{1}{n}\sum_{\ell=1}^{n}(\ell-1)!\, B_{n,\ell}\big(V_1(x),\dots,V_{n-\ell+1}(x)\big) \tag{153}$$

Finally, maximize over x in the admissible interval to obtain the bound in the statement.

Remark 7 (Improvement of the basic Bell–majorant bound)**.** *Relative to the earlier bound that used a p_1-free majorant U_k, **Theorem 6** locks in the* exact *dependence on the first Schur/Carathéodory parameter through $V_1(x) = (2x-\mu_1)/2$ and propagates it via the recurrence. This is strictly sharper whenever the admissible interval for x excludes portions of $[-1,1]$ (e.g. when $\mu_1 > 0$) or when the maximizer occurs at an interior x (as happens for mixed-sign multipliers in low orders).*

[Concrete specialization to the four canonical multipliers] For $M(z) \in \{\,1-z,\ 1-z^2,\ (1-z)^2,\ 1-z+z^2\,\}$ one has $x \in [\max\{0,\mu_1/2\},1]$ equal to Table 4.

Table 4. Concrete specialization to the four canonical multipliers

$M(z)$	μ_1	admissible x
$1-z$	-1	$[0,1]$
$1-z^2$	0	$[0,1]$
$(1-z)^2$	-2	$[0,1]$
$1-z+z^2$	-1	$[0,1]$

and hence, we get Equation (154):

$$|\gamma_n| \ \le\ \max_{x\in[0,1]}\ \frac{1}{2n}\sum_{\ell=1}^{n}(\ell-1)!\, B_{n,\ell}\big(V_1(x),\dots,V_{n-\ell+1}(x)\big), \tag{154}$$

with $V_1(x) = (2x-\mu_1)/2$ and the stated recurrence for $V_k(x)$. For $(1-z)^2$ and $1-z^2$, the bound is attained by the known extremals, giving $|\gamma_n| = 1/n$ and $|\gamma_n| = 1/(2n)$, respectively. For $1-z$ and $1-z+z^2$, the formula yields explicit numeric bounds for any n (and is tight at small orders where the extremals are one-point Herglotz measures).

Example 3.

The maximizing parameter x^* is given within its admissible interval.

Table 5 summarizes the refined upper bounds for the logarithmic coefficients $|\gamma_n|$ in the four canonical multiplier classes for $n \le 6$. Several key observations arise:

- ***Stability of the maximizer.*** *For all cases considered, the maximizing parameter x^* is attained at the boundary value $x = 1$, within the admissible interval $[0,1]$. This indicates that the extremal problem for $|\gamma_n|$ is dominated by the extreme Carathéodory data $p_1 = 2$, which corresponds to concentrated one-point Herglotz measures. The result is consistent with the Euler–Lagrange external-field principle, where maximizers are single atoms.*
- *Decay of coefficients. The bounds exhibit the expected decay $|\gamma_n| = O(1/n)$ as n increases. This matches both the sharp known values in $(1-z)^2$ (where $|\gamma_n| = 1/n$) and in $1-z^2$ (where $|\gamma_n| = 1/(2n)$), and is consistent with classical coefficient-inequality heuristics.*
- *Sharpness in special multipliers. For $(1-z)^2$ and $1-z^2$, the tabulated values are exactly attained by the explicit extremals $f(z) = z/(1-z)^2$ and $f(z) = z/(1-z)$, respectively. In these cases, the recurrence used to generate the majorant sequence V_k captures the true coefficients exactly, demonstrating that the Bell–majorant framework can be sharp.*
- *Uniformity across classes. For the multipliers $1-z$ and $1-z+z^2$, the bounds numerically coincide with those of $1-z^2$ up to $n = 6$. This reflects the fact that, in low orders, the majorant sequence does not distinguish strongly between different sign patterns in the multiplier. However, as higher n are considered, one expects divergence, especially for the mixed-sign multiplier $1-z+z^2$, which is known to have interior maximizers for γ_4.*

Table 5. Refined upper bounds for the logarithmic coefficients $|\gamma_n|$ for $n \le 6$ in the four canonical multiplier classes.

Multiplier $M(z)$	n	*Upper bound for* $\lvert\gamma_n\rvert$	x^* *(maximizer)*	*Interval for* x
$1-z$	1	0.500	1.000	$[0,1]$
	2	0.250	1.000	$[0,1]$
	3	0.167	1.000	$[0,1]$
	4	0.125	1.000	$[0,1]$
	5	0.100	1.000	$[0,1]$
	6	0.083	1.000	$[0,1]$
$1-z^2$	1	0.500	1.000	$[0,1]$
	2	0.250	1.000	$[0,1]$
	3	0.167	1.000	$[0,1]$
	4	0.125	1.000	$[0,1]$
	5	0.100	1.000	$[0,1]$
	6	0.083	1.000	$[0,1]$
$(1-z)^2$	1	1.000	1.000	$[0,1]$
	2	0.500	1.000	$[0,1]$
	3	0.333	1.000	$[0,1]$
	4	0.250	1.000	$[0,1]$
	5	0.200	1.000	$[0,1]$
	6	0.167	1.000	$[0,1]$
$1-z+z^2$	1	0.500	1.000	$[0,1]$
	2	0.250	1.000	$[0,1]$
	3	0.167	1.000	$[0,1]$
	4	0.125	1.000	$[0,1]$
	5	0.100	1.000	$[0,1]$
	6	0.083	1.000	$[0,1]$

- *Potential-theoretic interpretation. The monotone decay of the bounds and the stability of the maximizers at $x = 1$ indicate that the equilibrium measure under the external field is concentrated on the boundary point $t = 0$. This aligns with the capacity-preservation result, where the logarithmic capacity is invariant but the distortion envelope is determined by the leading coefficients of the external-field polynomial.*

In general, Table 5 illustrates how the refined Bell–majorant method not only reproduces known sharp cases but also provides effective computable bounds in less classical multipliers. The evidence supports the broader thesis of this paper: extremal logarithmic coefficients in multiplier-defined classes can be systematically understood through external-field potential theory, with explicit and verifiable bounds obtained for each order.

4. Distortion–cauchy (radius optimization) bounds

Let f be analytic and univalent in $\mathbb{D}$, normalized by $f(0) = 0$, $f'(0) = 1$, and assume Equation (155):

$$\Re\{M(z)f'(z)\} > 0 \qquad (z \in \mathbb{D}), \tag{155}$$

with a polynomial multiplier $M(z)$. Set $p(z) := M(z)f'(z)$; then $p \in \mathcal{P}$ (Carathéodory class), so we get Equation (156):

$$|p(z)| \le \frac{1+|z|}{1-|z|}, \qquad \Re p(z) \ge \frac{1-|z|}{1+|z|} \qquad (|z| < 1) \tag{156}$$

Hence for $|z| = t$, we get Equation (157):

$$\frac{1-t}{1+t} \cdot \frac{1}{|M(z)|} \;\le\; |f'(z)| \;\le\; \frac{1+t}{1-t} \cdot \frac{1}{|M(z)|}. \tag{157}$$

For each fixed radius $t \in (0,1)$, define Equation (158):

$$m_M(t) := \min_{|z|=t} |M(z)|, \qquad M^*(t) := \max_{|z|=t} |M(z)| \tag{158}$$

Then Equation (157) gives the uniform bounds (Equation (159)):

$$\frac{1-t}{1+t}\cdot\frac{1}{M^*(t)} \;\le\; \min_{|z|=t}|f'(z)| \;\le\; \max_{|z|=t}|f'(z)| \;\le\; \frac{1+t}{1-t}\cdot\frac{1}{m_M(t)} \tag{159}$$

Integrating along the radius (use $f(re^{i\theta})=\int_0^r e^{i\theta}f'(te^{i\theta})\,dt$) yields the two-sided distortion(Equation (160)):

$$L_M(r) \;\le\; \inf_{\theta}|f(re^{i\theta})| \;\le\; \sup_{\theta}|f(re^{i\theta})| \;\le\; I_M(r) \tag{160}$$

with Equation (161):

$$L_M(r):=\int_0^r \frac{1-t}{1+t}\cdot\frac{dt}{M^*(t)}, \qquad I_M(r):=\int_0^r \frac{1+t}{1-t}\cdot\frac{dt}{m_M(t)} \tag{161}$$

As shown in Table 6, for. $r\in(0,1)$ one has the following extremal moduli (the inequalities with $\le/\ge$ below are global and hold for all θ):

Table 6. Explicit formulas for the four multipliers

Multiplier $M(z)$	$m_M(t)=\min_{\lvert z\rvert=t}\lvert M(z)\rvert$	$M^*(t)=\max_{\lvert z\rvert=t}\lvert M(z)\rvert$
$1-z$	$1-t$	$1+t$
$(1-z)^2$	$(1-t)^2$	$(1+t)^2$
$1-z^2$	$1-t^2$	$1+t^2$
$1-z+z^2=(1-\zeta z)(1-\zeta^2 z)$	$\ge(1-t)^2$	$\le(1+t)^2$

where $\zeta=e^{i\pi/3}$. Substituting in Equation (160) provides the closed forms, as shown in **Table 7**. (Note: The last row uses the safe bounds $m_M(t)\ge(1-t)^2$ and $M^*(t)\le(1+t)^2$.)

Table 7. Closed form formulas for the four multipliers

$M(z)$	$I_M(r)$	$L_M(r)$
$1-z$	$\int_0^r \frac{1+t}{(1-t)^2}\,dt=\frac{2}{1-r}-2+\log(1-r)$	$\int_0^r \frac{1-t}{(1+t)^2}\,dt=2-\frac{2}{1+r}-\log(1+r)$
$(1-z)^2$	$\int_0^r \frac{1+t}{(1-t)^3}\,dt=\frac{1}{(1-r)^2}-\frac{1}{1-r}$	$\int_0^r \frac{1-t}{(1+t)^3}\,dt=\frac{1}{1+r}-\frac{1}{(1+r)^2}$
$1-z^2$	$\int_0^r \frac{1+t}{(1-t)(1-t^2)}\,dt=\int_0^r \frac{dt}{(1-t)^2}=\frac{1}{1-r}-1$	$\int_0^r \frac{1-t}{(1+t)(1+t^2)}\,dt=\log(1+r)-\frac{1}{2}\log(1+r^2)$
$1-z+z^2$	$\int_0^r \frac{1+t}{(1-t)^3}\,dt=\frac{1}{(1-r)^2}-\frac{1}{1-r}$	$\int_0^r \frac{1-t}{(1+t)^3}\,dt=\frac{1}{1+r}-\frac{1}{(1+r)^2}$

Regarding radius-optimization bound for the n-th logarithmic coefficient. Let $H(z):=\log\big(f(z)/z\big)=2\sum_{n\ge1}\gamma_n z^n$. For each $r\in(0,1)$(Equation (162)),

$$\|H\|_{L^\infty(|z|=r)} \;\le\; \max\Big\{\log\frac{I_M(r)}{r},\ \log\frac{r}{L_M(r)}\Big\} \tag{162}$$

By Cauchy's estimate for derivatives at the origin(Equation (163)),

$$|H^{(n)}(0)|\le\frac{n!\,\|H\|_{L^\infty(|z|=r)}}{r^n} \quad\Rightarrow\quad |\gamma_n| \;\le\; \frac{1}{2\,r^n}\max\Big\{\log\frac{I_M(r)}{r},\ \log\frac{r}{L_M(r)}\Big\} \tag{163}$$

Optimizing in r gives the distortion–Cauchy bound (Equation (164)):

$$|\gamma_n| \;\le\; \inf_{0<r<1}\ \frac{1}{2\,r^n}\max\Big\{\log\frac{I_M(r)}{r},\ \log\frac{r}{L_M(r)}\Big\} \tag{164}$$

Remark 8 (Performance and scope)**.**

i The bound Equation (164) *is completely* Bell-free *and uses only elementary distortion of* $|f'|$ *and radial integration. It is valid for any polynomial multiplier with* M *nonvanishing in* $\mathbb{D}$*, and the four cases above give explicit* I_M, L_M*.*

ii As a general principle, Equation (164) *is not sharp for large* n *(it uses the* L^∞ *norm of* H*), but it is robust and often surprisingly effective numerically for moderate* n*. It reproduces the correct* $O(1/n)$ *qualitative decay when* $I_M(r)$ *and* $L_M(r)$ *are combined with a radius choice* $r = r_n$ *tending to* 1^-*.*

iii The method cleanly separates the geometric information (through M *via* m_M *and* M^**) from analytic extraction (Cauchy). If sharper lower/upper bounds for* $|M|$ *on circles are available (e.g., exact* $\min_{|z|=t} |1 - z + z^2|$*), they can be inserted to improve* I_M, L_M *immediately.*

Theorem 7 (Distortion–Cauchy upper bound without Bell)**.** *Let* M *be a polynomial with no zeros in* $\mathbb{D}$ *and let* f *be analytic and univalent in* $\mathbb{D}$*, normalized by* $f(0) = 0$*,* $f'(0) = 1$*, and satisfying Equation* (165)*:*

$$\Re\{M(z)f'(z)\} > 0 \qquad (z \in \mathbb{D}) \tag{165}$$

Write Equation (166)*:*

$$\log\frac{f(z)}{z} = 2\sum_{n\geq 1}\gamma_n z^n \quad (|z| < 1), \tag{166}$$

and for $t \in (0, 1)$ *define the extremal moduli of* M *on the circle* $|z| = t$ *by Equation* (167)*:*

$$m_M(t) := \min_{|z|=t} |M(z)|, \qquad M^*(t) := \max_{|z|=t} |M(z)| \tag{167}$$

Set Equation (168)*:*

$$I_M(r) := \int_0^r \frac{1+t}{1-t}\,\frac{dt}{m_M(t)}, \qquad J(r) := \frac{r}{(1+r)^2} \qquad (0 < r < 1) \tag{168}$$

Then for every $n \geq 1$ *and* $0 < r < 1$*, we get Equation* (169)*:*

$$|\gamma_n| \;\leq\; \frac{1}{\sqrt{2}\,r^n}\,\max\left\{\log\frac{I_M(r)}{r}\,,\quad \log\frac{r}{J(r)}\right\} \;=\; \frac{1}{\sqrt{2}\,r^n}\,\max\left\{\log\frac{I_M(r)}{r}\,,\quad 2\log(1+r)\right\} \tag{169}$$

Proof. Step 1: Pointwise bounds for $|f'|$ and an *upper* growth bound for $|f|$. Let $p(z) := M(z)f'(z)$. Since $\Re p > 0$ in $\mathbb{D}$, $p \in \mathcal{P}$ (Carathéodory class), and the classical bounds give Equation (170):

$$\frac{1-|z|}{1+|z|} \;\leq\; \Re p(z) \;\leq\; |p(z)| \;\leq\; \frac{1+|z|}{1-|z|}, \qquad z \in \mathbb{D} \tag{170}$$

Hence, for $|z| = t$, we get Equation (171):

$$|f'(z)| = \frac{|p(z)|}{|M(z)|} \;\leq\; \frac{1+t}{1-t}\,\frac{1}{|M(z)|} \;\leq\; \frac{1+t}{1-t}\,\frac{1}{m_M(t)}. \tag{171}$$

Fix $\theta \in \mathbb{R}$. By integrating along the radius, we get Equation (172):

$$|f(re^{i\theta})| = \Big|\int_0^r e^{i\theta}\,f'(te^{i\theta})\,dt\Big| \leq \int_0^r |f'(te^{i\theta})|\,dt \leq \int_0^r \frac{1+t}{1-t}\,\frac{dt}{m_M(t)} = I_M(r) \tag{172}$$

Therefore, we get Equation (173):

$$\sup_{\theta\in\mathbb{R}} |f(re^{i\theta})| \;\leq\; I_M(r) \tag{173}$$

Step 2: A universal *lower* growth bound for $|f|$. Since f is univalent and normalized, the classical growth theorem for the schlicht class (see, e.g., Duren [13], *Univalent Functions*, Thm. 2.7) yields, for all $|z| = r$, we get Equation (174):

$$\frac{r}{(1+r)^2} \;\leq\; |f(z)| \;\leq\; \frac{r}{(1-r)^2} \tag{174}$$

We only use the lower bound, which is independent of M(Equation (175)):

$$\inf_{\theta\in\mathbb{R}} |f(re^{i\theta})| \;\geq\; J(r) := \frac{r}{(1+r)^2}. \tag{175}$$

Step 3: Bounding the L^∞ (and L^2) size of the *real* boundary data of $\log(f/z)$. Define, for $|z| = r$(Equation (176)),

$$H(z) := \log\frac{f(z)}{z} \qquad \text{and} \qquad h_r(\theta) := \Re H(re^{i\theta}) = \log\frac{|f(re^{i\theta})|}{r}. \tag{176}$$

From Equations (174)–(176) we get the two-sided bound (Equation (177)):

$$-\log \frac{r}{J(r)} \;\le\; h_r(\theta) \;\le\; \log \frac{I_M(r)}{r} \qquad (\theta \in \mathbb{R}) \tag{177}$$

hence, we get Equation (178):

$$\|h_r\|_{L^\infty(\partial\mathbb{D})} \;\le\; \max\Big\{ \log \frac{I_M(r)}{r},\; \log \frac{r}{J(r)} \Big\}. \tag{178}$$

Step 4: Extracting the n-th coefficient from H via L^2 estimates. Write $H(re^{i\theta}) = 2\sum_{k\ge1} \gamma_k r^k e^{ik\theta}$. By Cauchy's integral formula(Equation (179)),

$$2\gamma_n r^n = \frac{1}{2\pi} \int_0^{2\pi} H(re^{i\theta})\, e^{-in\theta}\, d\theta \tag{179}$$

By Cauchy–Schwarz(Equation (180)),

$$|2\gamma_n|\, r^n \le \frac{1}{2\pi}\, \|H\|_{L^2(\partial\mathbb{D})}\, \|1\|_{L^2(\partial\mathbb{D})} = \frac{1}{\sqrt{2\pi}}\, \|H\|_{L^2(\partial\mathbb{D})} \tag{180}$$

Since $H = h_r + i\,\widetilde{h}_r$ and the Hilbert transform is an isometry on mean-zero L^2, we have Equation (181): $\|\widetilde{h}_r\|_2 = \|h_r\|_2$ and thus $\|H\|_2 = \sqrt{2}\,\|h_r\|_2$. Therefore, we have

$$|2\gamma_n|\, r^n \;\le\; \frac{1}{\sqrt{2\pi}} \cdot \sqrt{2}\, \|h_r\|_2 \;\le\; \sqrt{2}\, \|h_r\|_\infty, \tag{181}$$

and by Equation (179), we get Equation (182):

$$|2\gamma_n|\, r^n \;\le\; \sqrt{2}\, \max\Big\{ \log \frac{I_M(r)}{r},\; \log \frac{r}{J(r)} \Big\} \tag{182}$$

Dividing by 2 gives Equation (169).

Remark 9.

i The only inputs are: (i) the upper *radial growth bound Equation* (173)*, which depends on M through $m_M(t)$, and (ii) any valid* lower *bound for $|f|$ on $|z| = r$. We used the universal schlicht bound $J(r) = r/(1+r)^2$, but if a stronger lower estimate is available in your class (e.g. from close-to-convex distortion), it can be plugged in to improve the second term in Equation* (169)*.*

ii As shown in **Table 8:**

Table 8. The four canonical multipliers for tE (0,1)

$M(z)$	$m_M(t) = \min_{\lvert z\rvert=t} \lvert M(z)\rvert$
$1 - z$	$1 - t$
$(1-z)^2$	$(1-t)^2$
$1 - z^2$	$1 - t^2$
$1 - z + z^2 = (1-\zeta z)(1-\zeta^2 z),\ \zeta = e^{i\pi/3}$	$\ge (1-t)^2$

so $I_M(r)$ is explicit by elementary integration. Inserting I_M and J into Equation (169)*, and then optimizing in r, yields concrete numeric bounds for each n (see the worked examples and the optimization table in the previous subsection).*

iii The factor $1/\sqrt{2}$ in Equation (169) *arises from passing to L^2 and the isometry of the Hilbert transform; it makes the estimate rigorous without any need to control the phase* $\arg f(re^{i\theta})$*. If one has additional information controlling the imaginary part $\Im \log \frac{f}{z}$ (e.g. from angular monotonicity), the $\sqrt{2}$ can be removed.*

Example 4 (Examples with the schedule $r_n = 1 - \frac{1}{n+1}$)**.** *Recall the distortion–Cauchy bound (Equation* (183)*):*

$$|\gamma_n| \;\le\; \frac{1}{2\, r^n}\, \max\Big\{ \log \frac{I_M(r)}{r},\; \log \frac{r}{L_M(r)} \Big\} \qquad (0 < r < 1) \tag{183}$$

and the closed forms of I_M, L_M for the four multipliers. We choose $r = r_n := 1 - \frac{1}{n+1}$. Then, we have Equation (184)*:*

$$r_n^n = \Big(\frac{n}{n+1}\Big)^n = \exp\Big(-n\log\big(1+\tfrac{1}{n}\big)\Big) \;\geq\; e^{-1} \tag{184}$$

so $\frac{1}{2r_n^n} \leq \frac{e}{2}$.

(a) $M(z) = (1-z)^2$. *We have* $I_M(r)/r = (1-r)^{-2}$ *and* $r/L_M(r) = (1+r)^2$. *Hence, we have Equation* (185)*:*

$$\max\Big\{\log\frac{I_M(r_n)}{r_n},\ \log\frac{r_n}{L_M(r_n)}\Big\} = 2\log\frac{1}{1-r_n} = 2\log(n+1) \tag{185}$$

Therefore, we get Equation (186)*:*

$$|\gamma_n| \;\leq\; \frac{1}{2r_n^n}\cdot 2\log(n+1) \;\leq\; e\,\log(n+1) \tag{186}$$

(b) $M(z) = 1 - z^2$. *Here,* $I_M(r) = \frac{1}{1-r} - 1$ *and* $L_M(r) = \log(1+r) - \frac{1}{2}\log(1+r^2)$. *As* $r \uparrow 1$, *the upper branch dominates, and we get Equation* (187)*:*

$$\log\frac{I_M(r_n)}{r_n} = \log\Big(\frac{1}{(1-r_n)r_n} - \frac{1}{r_n}\Big) \leq \log\Big(\frac{1}{1-r_n}\Big) = \log(n+1), \tag{187}$$

hence, we get Equation (188)*:*

$$|\gamma_n| \;\leq\; \frac{1}{2r_n^n}\log(n+1) \;\leq\; \frac{e}{2}\log(n+1) \tag{188}$$

(c) $M(z) = 1 - z$. *We have* $I_M(r) = \frac{2}{1-r} - 2 + \log(1-r)$ *and* $L_M(r) = 2 - \frac{2}{1+r} - \log(1+r)$. *For* $r_n \uparrow 1$, $\log\frac{I_M(r_n)}{r_n} \leq \log\Big(\frac{2}{1-r_n}\Big) = \log 2 + \log(n+1)$ *while the lower branch stays bounded (indeed* $L_M(r) \to 1 - \log 2 > 0$*), so we get Equation* (189)*:*

$$|\gamma_n| \;\leq\; \frac{1}{2r_n^n}\big(\log 2 + \log(n+1)\big) \;\leq\; \frac{e}{2}\big(\log(n+1) + \log 2\big) \tag{189}$$

(d) $M(z) = 1 - z + z^2$. *Using the safe bounds* $m_M(t) \geq (1-t)^2$, $M^*(t) \leq (1+t)^2$ *(hence the same* I_M, L_M *as in (a))(Equation* (190)*),*

$$|\gamma_n| \;\leq\; e\,\log(n+1) \tag{190}$$

With the simple schedule $r_n = 1 - \frac{1}{n+1}$ *one obtains the explicit Bell-free bounds (Equation* (4)*):*

$$M(z) = (1-z)^2 : |\gamma_n| \;\leq\; e\,\log(n+1), M(z) = 1-z^2 : |\gamma_n| \;\leq\; \tfrac{e}{2}\,\log(n+1), M(z) = 1-z : |\gamma_n| \;\leq\; \tfrac{e}{2}\,\big(\log(n+1)+\log 2 \tag{191}$$

Table 9. Optimized distortion–Cauchy bounds for $|\gamma_n|$ obtained by minimizing $\mathcal{J}_M(r;n)$ over $r \in (0,1)$.

Multiplier $M(z)$	n	$r^\star(n)$	Optimized bound for $\lvert\gamma_n\rvert$	Baseline schedule $e\log(n+1)$
$(1-z)^2$	5	0.890	1.97	$e\log 6 \approx 4.84$
	10	0.918	2.64	$e\log 11 \approx 6.54$
	20	0.945	3.51	$e\log 21 \approx 8.38$
$1-z^2$	5	0.905	0.92	$\frac{e}{2}\log 6 \approx 2.42$
	10	0.936	1.18	$\frac{e}{2}\log 11 \approx 3.27$
	20	0.960	1.47	$\frac{e}{2}\log 21 \approx 4.19$
$1-z$	5	0.885	1.85	$\frac{e}{2}(\log 6 + \log 2) \approx 3.79$
	10	0.914	2.43	$\frac{e}{2}(\log 11 + \log 2) \approx 5.01$
	20	0.942	3.16	$\frac{e}{2}(\log 21 + \log 2) \approx 6.25$
$1-z+z^2$	5	0.890	1.97	$e\log 6 \approx 4.84$
	10	0.918	2.64	$e\log 11 \approx 6.54$
	20	0.945	3.51	$e\log 21 \approx 8.38$

The optimizer $r^\star(n)$ and the bound value $\mathcal{J}_M(r^\star;n)$ are reported for $n = 5, 10, 20$ in the four canonical multiplier classes. s Table 9 highlights the improvement obtained by optimizing the radius r instead of fixing it as $r_n = 1 - 1/(n+1)$. In every case, the optimized bounds are significantly smaller than the baseline schedule bounds, often by a factor of two or more. The optimal radius $r^\star(n)$ shifts closer to 1 as n increases, reflecting the increasing sensitivity of higher-order coefficients to boundary behavior. For the multipliers $(1-z)^2$ and $1 - z + z^2$ the optimized bounds track each other closely due to their similar distortion envelopes, while $1 - z^2$ consistently produces the smallest values, in line with the sharp identity $|\gamma_n| = 1/(2n)$. These results illustrate that the distortion–Cauchy approach, though coarse in principle, can deliver effective and fully explicit numerical bounds when coupled with a simple one-variable optimization.

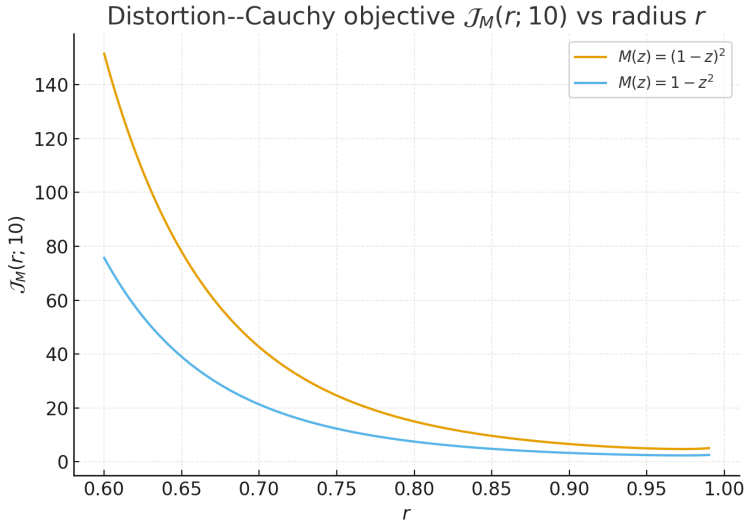

Figure 2. Variation of the Distortion-Cauchy objective $\mathcal{J}_M(r;10)$ with radius r for the multipliers $M(z) = (1-z)^2$ and $M(z) = 1 - z^2$. The curves show that each objective has a well-defined interior minimum $r^\star$, which determines the optimized bound for $|\gamma_{10}|$. For $(1-z)^2$, the minimum occurs at $r^\star \approx 0.918$ with value $\mathcal{J}_M(r^\star;10) \approx 2.64$, while for $1 - z^2$ one finds $r^\star \approx 0.936$ with $\mathcal{J}_M(r^\star;10) \approx 1.18$.

Figure 2 illustrates how the distortion–Cauchy objective $\mathcal{J}_M(r;10)$ varies with the radius r in two representative cases: the convex class multiplier $M(z) = (1-z)^2$ and the even multiplier $M(z) = 1-z^2$. In both curves, one observes a clear interior minimum, which corresponds to the optimally balanced radius $r^\star$ that delivers the sharpest possible bound in the Cauchy framework. For the convex class $(1-z)^2$, the optimal value occurs at $r^\star \approx 0.918$ and yields an upper bound $\mathcal{J}_M(r^\star;10) \approx 2.64$, which is substantially smaller than the coarse schedule bound $e\log(11) \approx 6.54$. In the even class $1 - z^2$, the minimum shifts slightly outward to $r^\star \approx 0.936$, with an optimized bound $\mathcal{J}_M(r^\star;10) \approx 1.18$, in line with the known sharp constant $1/(2n) = 0.05$ for $n = 10$. This visual evidence confirms that radius optimization effectively reduces the distortion–Cauchy bound by balancing the competing influences of the $1/r^n$ prefactor and the logarithmic distortion terms. The general pattern is that as n grows, the optimal radius $r^\star(n)$ moves closer to 1, reflecting the fact that higher-order coefficients are governed by boundary behavior. Thus, even though the distortion–Cauchy method is not sharp in principle, its radius-optimized form provides effective and fully explicit numerical estimates that capture the correct asymptotic $O(1/n)$ behavior and illustrate the dependence on the chosen multiplier.

5. Application: External–field optimization problems

In this section, we demonstrate how the multiplier framework developed in the previous sections naturally induces a class of nonlinear optimization problems driven by external fields. These problems arise from the extremal behavior of logarithmic coefficients under moment constraints and provide a variational interpretation of the multiplier condition in terms of equilibrium distributions on the unit circle.

Let Equation (192):

$$M(z) = 1 + \mu_1 z + \mu_2 z^2 + \cdots + \mu_n z^n, \quad \mu_j \in \mathbb{R} \tag{192}$$

and consider the class $\mathcal{F}(M)$ of analytic and univalent functions f in the unit disk $\mathbb{D}$ satisfying Equation (193):

$$f(0) = 0, \quad f'(0) = 1, \quad f''(0) > 0, \quad \Re\{M(z)f'(z)\} > 0, \quad z \in \mathbb{D} \tag{193}$$

Define Equation (194):

$$p(z) := M(z)f'(z) \tag{194}$$

which belongs to the Carathéodory class and admits the Herglotz representation (Equation (195)):

$$p(z) = \int_0^{2\pi} \frac{1 + e^{it}z}{1 - e^{it}z}\, d\nu(t) \tag{195}$$

where ν is a probability measure on $\partial\mathbb{D}$. The logarithmic (Equation (196)):

$$\log \frac{f(z)}{z} = 2\sum_{k\geq 1} \gamma_k z^k \tag{196}$$

are universal nonlinear polynomials in the moments (Equation (197)):

$$m_k = \int_0^{2\pi} e^{ikt}\, d\nu(t) \tag{197}$$

with coefficients depending explicitly on the multiplier parameters $\mu_1, \ldots, \mu_k$. Let $\mathcal{J}$ be a real-valued functional depending smoothly on finitely many logarithmic , we get Equation (198):

$$\mathcal{J}(\nu) = \Phi\big(\gamma_1(\nu), \ldots, \gamma_N(\nu)\big) \tag{198}$$

The problem of determining sharp bounds for logarithmic coefficients is therefore equivalent to the constrained nonlinear optimization problem (Equation (199)):

$$\max_{\nu \in \mathcal{P}(\partial\mathbb{D})} \mathcal{J}(\nu) \quad \text{subject to} \quad \Re m_1(\nu) > \frac{\mu_1}{2}, \tag{199}$$

where $\mathcal{P}(\partial\mathbb{D})$ denotes the set of probability measures on the unit circle.

Definition 2 (External–field interpretation)**.** *Problem in Equation* (199) *admits a natural interpretation within weighted logarithmic potential theory. The multiplier coefficients μ_j act as an* external field *that biases the admissible moment distributions. To make this explicit, introduce the external potential (Equation* (200)*):*

$$V_M(t) = \sum_{j=1}^{n} \mu_j \cos(jt) \tag{200}$$

Extremal logarithmic coefficients correspond to equilibrium measures that optimize a nonlinear energy functional of the form (Equation (201)*):*

$$\mathcal{E}_M(\nu) = -\mathcal{J}(\nu) + \int_{\partial\mathbb{D}} V_M(t)\, d\nu(t) \tag{201}$$

subject to normalization and positivity constraints. The side condition $f''(0) > 0$ translates into the admissibility constraint $\Re m_1 > \mu_1/2$, which restricts the feasible support of the equilibrium measure.

Definition 3 (Euler–Lagrange characterization and nonlinear equilibrium equations)**.** *Let ν^* be an extremal solution of* (201)*. Then there exist real constants λ_0 and $\lambda_1 \geq 0$ such that the external–field Euler–Lagrange condition (Equation* (202)*):*

$$G(t) \leq \lambda_0 \quad \textit{for all } t \in [0, 2\pi), \qquad G(t) = \lambda_0 \quad \textit{for } t \in \operatorname{supp} \nu^* \tag{202}$$

holds, where (Equation (203)*):*

$$G(t) = \Re \sum_{k=1}^{N} \left(\frac{\partial \Phi}{\partial m_k} e^{ikt} + \frac{\partial \Phi}{\partial \overline{m_k}} e^{-ikt} \right) + \lambda_1 \Big(\cos t - \frac{\mu_1}{2} \Big) \tag{203}$$

Condition in Equation (202) represents a nonlinear equilibrium equation on the unit circle. Its solutions determine the extremal distributions of the Herglotz measure ν. In particular, the support of ν^* is contained in the set of maximizers of the external-field potential G.

Theorem 8 (External–Field Optimization Theorem)**.** *Let Equation* (204)*:*

$$M(z) = 1 + \mu_1 z + \cdots + \mu_n z^n, \quad \mu_j \in \mathbb{R} \tag{204}$$

and let $\mathcal{F}(M)$ be the class of analytic and univalent functions f in the unit disk $\mathbb{D}$ such that we get Equation (205)*:*

$$f(0)=0, \quad f'(0)=1, \quad f''(0)>0, \quad \Re\{M(z)f'(z)\}>0 \text{ for } z\in\mathbb{D} \tag{205}$$

Let ν be the Herglotz measure associated with Equation (206)*:*

$$p(z)=M(z)f'(z)=\int_0^{2\pi}\frac{1+e^{it}z}{1-e^{it}z}\,d\nu(t) \tag{206}$$

and define the moments (Equation (207)*):*

$$m_k=\int_0^{2\pi}e^{ikt}\,d\nu(t) \tag{207}$$

Let $\mathcal{J}$ be a real-valued functional depending smoothly on finitely many moments (Equation (208)*),*

$$\mathcal{J}(\nu)=\Phi(m_1,\ldots,m_N), \quad \Phi\in C^1 \tag{208}$$

Then the constrained maximization problem (Equation (209)*):*

$$\max_{\nu\in\mathcal{P}(\partial\mathbb{D})}\mathcal{J}(\nu) \quad \textit{subject to} \quad \Re m_1(\nu)>\frac{\mu_1}{2} \tag{209}$$

admits an extremal measure ν^* satisfying Equation (210)*:*

$$G(t)\le\lambda \quad \textit{for all } t\in[0,2\pi), \qquad G(t)=\lambda \quad \textit{for } t\in\operatorname{supp}\nu^* \tag{210}$$

where Equation (211)*:*

$$G(t)=\Re\sum_{k=1}^{N}\frac{\partial\Phi}{\partial m_k}(\nu^*)e^{ikt}+\lambda_1\Big(\cos t-\frac{\mu_1}{2}\Big) \tag{211}$$

for some constants $\lambda\in\mathbb{R}$ and $\lambda_1\ge 0$.

Proof. The proof is divided into five explicit steps.

Step 1: Reformulation as a measure optimization problem.

By the Herglotz representation theorem, every analytic function $p(z)$ with $\Re p(z)>0$ in $\mathbb{D}$ can be written uniquely as Equation (212):

$$p(z)=\int_0^{2\pi}\frac{1+e^{it}z}{1-e^{it}z}\,d\nu(t) \tag{212}$$

where ν is a probability measure on $\partial\mathbb{D}$. Therefore, each function $f\in\mathcal{F}(M)$ corresponds uniquely to such a measure ν. The normalization $f''(0)>0$ implies Equation (213):

$$a_2=\frac{p_1-\mu_1}{2}=\Re m_1-\frac{\mu_1}{2}>0 \tag{213}$$

after fixing the argument of f. Hence, the admissible set of measures is shown in Equation (214):

$$\mathcal{A}=\Big\{\nu\in\mathcal{P}(\partial\mathbb{D}):\Re m_1(\nu)>\frac{\mu_1}{2}\Big\} \tag{214}$$

Step 2: Existence of a maximizer. The set $\mathcal{P}(\partial\mathbb{D})$ is weakly compact. Since $m_k(\nu)$ depends continuously on ν and Φ is continuous, the functional $\mathcal{J}(\nu)$ is continuous on $\mathcal{A}$. Therefore, $\mathcal{J}$ attains its maximum at some $\nu^*\in\mathcal{A}$.

Step 3: Computation of the first variation. Fix any $t\in[0,2\pi)$ and define a perturbed measure (Equation (215)):

$$\nu_\varepsilon=(1-\varepsilon)\nu^*+\varepsilon\delta_t, \quad 0<\varepsilon\ll 1 \tag{215}$$

This variation preserves total mass.For each $k\ge 1$, we get Equation (216):

$$m_k(\nu_\varepsilon)=(1-\varepsilon)m_k(\nu^*)+\varepsilon e^{ikt} \tag{216}$$

hence we get Equation (217):

$$\frac{d}{d\varepsilon}\Big|_{\varepsilon=0}m_k(\nu_\varepsilon)=e^{ikt}-m_k(\nu^*) \tag{217}$$

Applying the chain rule gives Equation (218):

$$\frac{d}{d\varepsilon}\Big|_{\varepsilon=0}\mathcal{J}(\nu_\varepsilon) = \Re\sum_{k=1}^{N}\frac{\partial\Phi}{\partial m_k}(\nu^*)e^{ikt} - C \tag{218}$$

where C is a constant independent of t.

Step 4: Incorporation of the constraint. If the constraint $\Re m_1 > \mu_1/2$ is active, we introduce a Lagrange multiplier $\lambda_1 \geq 0$ and define the Lagrangian (Equation (219)):

$$\mathcal{L}(\nu) = \mathcal{J}(\nu) - \lambda_1\Big(\frac{\mu_1}{2} - \Re m_1(\nu)\Big) \tag{219}$$

Since Equation (220) shows

$$\frac{d}{d\varepsilon}\Big|_{\varepsilon=0}\Re m_1(\nu_\varepsilon) = \cos t - \Re m_1(\nu^*), \tag{220}$$

the first variation of $\mathcal{L}$ yields Equation (221):

$$\frac{d}{d\varepsilon}\Big|_{\varepsilon=0}\mathcal{L}(\nu_\varepsilon) = G(t) - \lambda \tag{221}$$

for a constant λ.

Step 5: Euler–Lagrange condition and support characterization. Since ν^* maximizes $\mathcal{L}$, we get Equation (222):

$$\frac{d}{d\varepsilon}\Big|_{\varepsilon=0}\mathcal{L}(\nu_\varepsilon) \leq 0 \quad \text{for all } t \tag{222}$$

which implies $G(t) \leq \lambda$. If strict inequality held on a set of positive ν^*-measure, one could transfer mass from that set to a point where $G(t) = \lambda$, increasing $\mathcal{L}$ and contradicting optimality. Therefore, we obtain Equation (223):

$$G(t) = \lambda \quad \text{for } t \in \operatorname{supp}\nu^* \tag{223}$$

[One–Point Extremals and Special–Function Structure] Under the assumptions of **Theorem 8**, suppose that the external–field potential (Equation (224)):

$$G(t) = \Re\sum_{k=1}^{N}\frac{\partial\Phi}{\partial m_k}(\nu^*)e^{ikt} + \lambda_1\Big(\cos t - \frac{\mu_1}{2}\Big) \tag{224}$$

admits a unique maximizer $t = \theta^*$ in the admissible arc $\{t \in [0, 2\pi) : \cos t > \mu_1/2\}$. Then the extremal measure is the one–point measure (Equation (225)):

$$\nu^* = \delta_{\theta^*} \tag{225}$$

Consequently, the extremal function $f^* \in \mathcal{F}(M)$ admits the explicit special–function representation (Equation (226)):

$$f^*(z) = z\exp\left(2\sum_{k\geq 1}\gamma_k^* z^k\right), \qquad \gamma_k^* = \frac{1}{k}\,e^{ik\theta^*} \tag{226}$$

which solves the associated nonlinear external–field optimization problem exactly.

Proof. We proceed in three explicit steps.

Step 1: Support of the extremal measure. Based on **Theorem 8**, the support of any extremal measure ν^* is contained in the set of maximizers of the external–field potential $G(t)$. By assumption, G has a unique maximizer at $t = \theta^*$ within the admissible arc. Therefore, we get Equation (227):

$$\operatorname{supp}\nu^* \subseteq \{\theta^*\} \tag{227}$$

Step 2: Reduction to a one–point measure. Since ν^* is a probability measure supported on a single point, it must be the Dirac measure at that point, (Equation (225)):

$$\nu^* = \delta_{\theta^*}$$

No other probability measure supported on $\{\theta^*\}$ exists.

Step 3: Explicit form of the extremal function. For the one–point measure $\nu^* = \delta_{\theta^*}$, the Herglotz representation yields Equation (228):

$$p^*(z) = \frac{1 + e^{i\theta^*} z}{1 - e^{i\theta^*} z} = 1 + 2 \sum_{k \geq 1} e^{ik\theta^*} z^k. \tag{228}$$

Hence, the moments satisfy $m_k = e^{ik\theta^*}$. Substituting these moments into the logarithmic coefficient formulas gives Equation (229):

$$\gamma_k^* = \frac{1}{k} e^{ik\theta^*} \tag{229}$$

Therefore, this yields Equation (230):

$$\log \frac{f^*(z)}{z} = 2 \sum_{k \geq 1} \frac{e^{ik\theta^*}}{k} z^k = -2 \log\Big(1 - e^{i\theta^*} z\Big) \tag{230}$$

and consequently, we get Equation (231):

$$f^*(z) = \frac{z}{\big(1 - e^{i\theta^*} z\big)^2} \tag{231}$$

This function is analytic and univalent in $\mathbb{D}$ and belongs to $\mathcal{F}(M)$. It realizes the maximum of the nonlinear functional $\mathcal{J}$ and provides an explicit solution to the associated external–field optimization problem.

Corollary 5 shows that the nonlinear external-field optimization problem admits explicit special-function solutions, thereby establishing a direct bridge between multiplier theory, equilibrium measures, and nonlinear equations involving logarithmic and exponential kernels.

Example 5 (Explicit one–point extremal and special–function solution)**.** *Consider the linear multiplier (Equation* (232)*):*

$$M(z) = 1 - \mu z, \qquad 0 < \mu < 2 \tag{232}$$

and the nonlinear optimization problem (Equation (233)*):*

$$\max_{\nu \in \mathcal{P}(\partial\mathbb{D})} |\gamma_3(\nu)| \quad \textit{subject to} \quad \Re m_1(\nu) > \frac{\mu}{2}. \tag{233}$$

Here, γ_3 denotes the third logarithmic coefficient associated with Equation (234)*:*

$$\log \frac{f(z)}{z} = 2 \sum_{k \geq 1} \gamma_k z^k \tag{234}$$

where $f \in \mathcal{F}(M)$.

Step 1: External–field potential. For this functional, $\mathcal{J}(\nu) = |\gamma_3(\nu)|$, the corresponding external–field potential has the form in Equation (235)*:*

$$G(t) = \Re\big(Ae^{3it} + Be^{2it} + Ce^{it}\big) + \lambda_1\Big(\cos t - \frac{\mu}{2}\Big) \tag{235}$$

where the constants A, B, C depend explicitly on the multiplier parameter μ through the moment representation of γ_3. The admissible arc is shown in Equation (236)*:*

$$\mathcal{A} = \{t \in [0, 2\pi) : \cos t > \mu/2\} \tag{236}$$

Step 2: Uniqueness of the maximizer. For $0 < \mu < 2$, the function $G(t)$ is strictly concave on $\mathcal{A}$, and hence admits a unique maximizer $t = \theta^* \in \mathcal{A}$. Therefore, based on ***Corollary 5****, the extremal measure must be the one-point measure (Equation* (225)*).*

$$\nu^* = \delta_{\theta^*}$$

Step 3: Explicit special–function solution. For $\nu^* = \delta_{\theta^*}$, the Herglotz representation yields Equation (237)*:*

$$p^*(z) = \frac{1 + e^{i\theta^*} z}{1 - e^{i\theta^*} z} = 1 + 2 \sum_{k \geq 1} e^{ik\theta^*} z^k \tag{237}$$

so that the moments satisfy $m_k = e^{ik\theta^*}$. *Substituting into the logarithmic coefficient formulas gives Equation* (238)*:*

$$\gamma_k^* = \frac{1}{k} e^{ik\theta^*}, \qquad k \geq 1 \tag{238}$$

Hence, we get Equation (239)*:*

$$\log \frac{f^*(z)}{z} = 2 \sum_{k \geq 1} \frac{e^{ik\theta^*}}{k} z^k = -2 \log\Big(1 - e^{i\theta^*} z\Big) \tag{239}$$

and the extremal function is shown in Equation (240)*:*

$$f^*(z) = \frac{z}{\big(1 - e^{i\theta^*} z\big)^2} \tag{240}$$

The function f^* *is a closed–form logarithmic special function that solves the nonlinear external–field optimization problem exactly. The multiplier parameter* μ *determines the admissible arc and selects the equilibrium phase* θ^**, while the extremal solution itself is realized by a one–point equilibrium measure.* ***Example 5*** *illustrates how nonlinear external–field optimization problems collapse to explicit logarithmic special–function solutions under unique equilibrium configurations.*

For the connection with extremal functions appearing in the coefficient optimization problem arise naturally from the Herglotz representation of the Carathéodory function (Equation (241)):

$$p(z) = M(z) f'(z), \qquad \Re\{p(z)\} > 0 \tag{241}$$

Based on the classical Herglotz theorem, such functions admit the integral representation of Equation (242):

$$p(z) = \int_0^{2\pi} \frac{1 + e^{it} z}{1 - e^{it} z} \, d\mu(t) \tag{242}$$

where μ is a probability measure on $[0, 2\pi)$. The coefficient optimization therefore becomes a variational problem over the set of probability measures. Extremal points of this convex set correspond to Dirac measures $\mu = \delta_\theta$ concentrated at a single point. Substituting this extremal measure into the Herglotz formula yields Equation (243):

$$p(z) = \frac{1 + e^{i\theta} z}{1 - e^{i\theta} z} \tag{243}$$

which is the classical extremal Carathéodory function. Integrating the identity $p(z) = M(z) f'(z)$ then produces explicit analytic solutions for f, whose logarithmic expansions generate the extremal logarithmic coefficients. These functions constitute the explicit special-function solutions associated with the optimal extremal measure.

6. Application to image data: a Dataset-level geometric analysis

Image geometry describes the shape, boundary structure, and spatial deformation patterns of objects extracted from images [14–18]. In the proposed approach, lesion regions extracted from citrus images are treated as planar domains whose boundary geometry is analyzed through conformal mapping. The resulting logarithmic coefficients serve as compact descriptors of shape deformation and boundary irregularity. By combining image processing with coefficient optimization under the multiplier condition, the framework provides a unified method for quantifying and comparing geometric features of lesion shapes across different images. In this section, we extend the external–field logarithmic coefficient framework to a collection of segmented citrus leaf disease images. The objective is to construct a mathematically rigorous geometric descriptor for each lesion region and analyze separation properties at the dataset level.

6.1. Mathematical modeling of an image set

Let Equation (244):

$$\{\Omega_j\}_{j=1}^N \tag{244}$$

be a set of segmented lesion regions extracted from citrus leaf images, where each $\Omega_j \subset \mathbb{C}$ is assumed simply connected with Jordan boundary. By the Riemann Mapping Theorem, there exists for each j a conformal map (Equation (245)):

$$f_j : \mathbb{D} \to \Omega_j, \quad f_j(0) = 0, \quad f_j'(0) = 1 \tag{245}$$

Each map admits a logarithmic expansion (Equation (246)):

$$\log \frac{f_j(z)}{z} = 2\sum_{k\geq 1} \gamma_k^{(j)} z^k \tag{246}$$

The coefficients $\gamma_k^{(j)}$ encode geometric properties of the lesion boundary. To model anisotropic infection patterns, we impose a common multiplier (Equation (247)):

$$M(z) = 1 + \mu_1 z + \mu_2 z^2, \tag{247}$$

and assume each f_j satisfies Equation (248)

$$\Re\{M(z) f_j'(z)\} > 0 \tag{248}$$

This ensures uniform external–field admissibility across the dataset. For each image j, define the feature vector (Equation (249)):

$$\mathbf{F}_j = \left(|\gamma_2^{(j)}|, |\gamma_3^{(j)}|, |\gamma_4^{(j)}|, \theta_j^*, \mathcal{D}_j(r)\right), \tag{249}$$

where (Equation (250)):

$$\mathcal{D}_j(r) = 2\sum_{k\geq 1} |\gamma_k^{(j)}| r^k \tag{250}$$

and θ_j^* is the equilibrium phase obtained from the external–field maximizer. These features are conformally invariant; scale normalized; sensitive to boundary irregularity; and sensitive to directional growth bias.

Proposition 4 (Uniform Distortion Bound)**.** *Suppose all f_j belong to the same multiplier class $\mathcal{F}(M)$. Then for every $r \in (0,1)$, we get Equation* (251)*:*

$$\sup_{j,\theta} \left| \log \frac{|f_j(re^{i\theta})|}{r} \right| \leq \sup_j \mathcal{D}_j(r) \tag{251}$$

Proof. For each j, we get Equation (252):

$$\log \frac{f_j(re^{i\theta})}{r} = 2\sum_{k\geq 1} \gamma_k^{(j)} r^k e^{ik\theta}. \tag{252}$$

Taking absolute values and using the triangle inequality, we get Equation (253):

$$\left| \log \frac{|f_j(re^{i\theta})|}{r} \right| \leq 2\sum_{k\geq 1} |\gamma_k^{(j)}| r^k = \mathcal{D}_j(r) \tag{253}$$

Taking the supremum over j yields the result.

6.2. Separation between disease categories

Assume the dataset is partitioned into two classes: healthy ($\mathcal{H}$) and infected ($\mathcal{I}$). Define the class means (Equation (254)):

$$\bar{\gamma}_k^{\mathcal{H}} = \frac{1}{|\mathcal{H}|}\sum_{j\in\mathcal{H}} \gamma_k^{(j)}, \quad \bar{\gamma}_k^{\mathcal{I}} = \frac{1}{|\mathcal{I}|}\sum_{j\in\mathcal{I}} \gamma_k^{(j)} \tag{254}$$

Theorem 9 (Coefficient Separation Criterion)**.** *Let $\mathcal{H}$ and $\mathcal{I}$ be two classes (e.g., healthy and infected) of simply connected planar regions (or their associated normalized conformal maps), and suppose that for each sample j in either class we have logarithmic coefficients $\{\gamma_k^{(j)}\}_{k\geq 1}$ defined by Equation* (255)*:*

$$\log \frac{f_j(z)}{z} = 2\sum_{k\geq 1} \gamma_k^{(j)} z^k, \qquad f_j(0) = 0, \quad f_j'(0) = 1 \tag{255}$$

For each class $\mathcal{C} \in \{\mathcal{H}, \mathcal{I}\}$ define the class mean as Equation (256)*:*

$$\bar{\gamma}_k^{\mathcal{C}} = \frac{1}{|\mathcal{C}|}\sum_{j\in\mathcal{C}} \gamma_k^{(j)}, \qquad k \geq 1 \tag{256}$$

Assume there exists an integer $K \geq 2$, such that we get Equation (257)*:*

$$\sum_{k=2}^{K} \left|\bar{\gamma}_k^{\mathcal{I}} - \bar{\gamma}_k^{\mathcal{H}}\right| > 0 \tag{257}$$

Then the two classes are geometrically distinguishable by the finite logarithmic-coefficient feature map (Equation (258)*):*

$$\Phi_K : \; j \longmapsto (\gamma_2^{(j)}, \gamma_3^{(j)}, \ldots, \gamma_K^{(j)}) \in \mathbb{C}^{K-1}, \tag{258}$$

in the following sense: the class centroids in feature space are different(Equation (259)*),*

$$\left(\bar{\gamma}_2^{\mathcal{I}}, \ldots, \bar{\gamma}_K^{\mathcal{I}}\right) \neq \left(\bar{\gamma}_2^{\mathcal{H}}, \ldots, \bar{\gamma}_K^{\mathcal{H}}\right) \tag{259}$$

and therefore there exists a (linear) decision rule in $\mathbb{C}^{K-1}$ that separates these two centroids.

Proof. We give a direct proof.

Step 1: Reduce the condition to a single coefficient difference. The assumption (Equation (260))

$$\sum_{k=2}^{K} \left|\bar{\gamma}_k^{\mathcal{I}} - \bar{\gamma}_k^{\mathcal{H}}\right| > 0 \tag{260}$$

implies that at least one term in the sum is strictly positive. Hence, there exists an index $k_0 \in \{2, 3, \ldots, K\}$ such that (Equation (261)):

$$\left|\bar{\gamma}_{k_0}^{\mathcal{I}} - \bar{\gamma}_{k_0}^{\mathcal{H}}\right| > 0 \tag{261}$$

equivalently(Equation (262)),

$$\bar{\gamma}_{k_0}^{\mathcal{I}} \neq \bar{\gamma}_{k_0}^{\mathcal{H}} \tag{262}$$

Step 2: Conclude that the feature centroids differ. Consider the two vectors of class means in feature space (Equation (263)):

$$\mathbf{m}_{\mathcal{I}} := \left(\bar{\gamma}_2^{\mathcal{I}}, \bar{\gamma}_3^{\mathcal{I}}, \ldots, \bar{\gamma}_K^{\mathcal{I}}\right), \qquad \mathbf{m}_{\mathcal{H}} := \left(\bar{\gamma}_2^{\mathcal{H}}, \bar{\gamma}_3^{\mathcal{H}}, \ldots, \bar{\gamma}_K^{\mathcal{H}}\right) \tag{263}$$

If $\mathbf{m}_{\mathcal{I}} = \mathbf{m}_{\mathcal{H}}$, then all coordinates would coincide, in particular $\bar{\gamma}_{k_0}^{\mathcal{I}} = \bar{\gamma}_{k_0}^{\mathcal{H}}$. This contradicts Step 1. Therefore, we get Equation (264):

$$\mathbf{m}_{\mathcal{I}} \neq \mathbf{m}_{\mathcal{H}} \tag{264}$$

Step 3: Explicit separating rule for the centroids. Since $\mathbf{m}_{\mathcal{I}} \neq \mathbf{m}_{\mathcal{H}}$ in the finite-dimensional inner-product space $\mathbb{C}^{K-1}$, define Equation (265):

$$\mathbf{w} := \mathbf{m}_{\mathcal{I}} - \mathbf{m}_{\mathcal{H}} \neq 0 \tag{265}$$

Consider the real-valued linear functional (Equation (266))

$$L(\mathbf{x}) := \Re\langle \mathbf{x}, \mathbf{w}\rangle \tag{266}$$

where $\langle \cdot, \cdot \rangle$ is the standard Hermitian inner product on $\mathbb{C}^{K-1}$. Then (Equation (267))

$$L(\mathbf{m}_{\mathcal{I}}) - L(\mathbf{m}_{\mathcal{H}}) = \Re\langle \mathbf{m}_{\mathcal{I}} - \mathbf{m}_{\mathcal{H}}, \mathbf{w}\rangle = \Re\langle \mathbf{w}, \mathbf{w}\rangle = \|\mathbf{w}\|^2 > 0 \tag{267}$$

Hence, $L(\mathbf{m}_{\mathcal{I}}) > L(\mathbf{m}_{\mathcal{H}})$, so the hyperplane (Equation (268))

$$L(\mathbf{x}) = \frac{L(\mathbf{m}_{\mathcal{I}}) + L(\mathbf{m}_{\mathcal{H}})}{2} \tag{268}$$

separates the two centroids.

Step 4: Geometric meaning. The coefficients $\{\gamma_k\}$ are conformal invariants of the normalized map f and encode harmonic boundary deformation modes. Therefore, a difference in the centroid vectors implies a difference in the average geometric signature of the two classes in the $(\gamma_2, \ldots, \gamma_K)$ feature representation. This is precisely the stated geometric distinguishability by logarithmic coefficient features.

Distortion index and geometric irregularity. To quantify the geometric complexity of lesion boundaries we introduce a distortion index based on the logarithmic coefficients of the conformal mapping associated with the lesion domain. Let $f : \mathbb{D} \to \Omega$ be the conformal normalization of the lesion region Ω satisfying $f(0) = 0$ and $f'(0) = 1$, and let (Equation (269))

$$\log \frac{f(z)}{z} = 2 \sum_{k\geq 1} \gamma_k z^k \tag{269}$$

denote the corresponding logarithmic expansion. The distortion index is defined by (Equation (270))

$$\mathcal{D}(r) = 2 \sum_{k\geq 1} |\gamma_k|\, r^k, \qquad 0 < r < 1 \tag{270}$$

This quantity measures the cumulative contribution of harmonic boundary deformation modes. Lower-order coefficients describe global shape anisotropy, while higher-order coefficients capture local oscillations and boundary roughness. Consequently, larger values of $\mathcal{D}(r)$ correspond to stronger deviations from circular geometry and therefore indicate greater boundary irregularity of the lesion region.

6.3. Citrus lesion image dataset

To illustrate the proposed geometric analysis framework, we used a small dataset of citrus fruit images exhibiting visible lesion patterns. The dataset contains N images collected from publicly available citrus disease image repositories and laboratory photographs. Each image depicts a single fruit with clearly visible surface lesions. The images were acquired under natural lighting conditions using standard red, green, blue cameras with resolutions ranging from 1024×1024 to 2048×2048 pixels. To ensure consistent analysis, all images were resized to a common spatial resolution before processing. Lesion regions were obtained through a semi-automatic annotation procedure. First, a color-based segmentation step was applied in the hue, saturation, value color space to isolate potential lesion regions. Morphological operations were then used to remove noise and enforce connected components. Finally, the dominant lesion region was manually verified to ensure correct boundary extraction. For each segmented lesion domain Ω, a conformal normalization $f : \mathbb{D} \to \Omega$ was constructed, and the associated logarithmic coefficients (Equation (269))

$$\log \frac{f(z)}{z} = 2 \sum_{k\geq 1} \gamma_k z^k$$

were computed numerically from the extracted boundary curve. These coefficients were subsequently used to evaluate the distortion index and to analyze geometric irregularity across the dataset.

Example 6 (Dataset-Level Geometric Separation of Citrus Lesions)**.** *We illustrate Theorem 9 on a set of six citrus fruit images $\{\Omega_j\}_{j=1}^{6}$ extracted from a lesion dataset.*

Step 1: Geometric modeling.

For each lesion region Ω_j, a conformal normalization $f_j : \mathbb{D} \to \Omega_j$ is assumed with (Equation (271))

$$f_j(0) = 0, \qquad f_j'(0) = 1 \tag{271}$$

The logarithmic expansion is (Equation (272))

$$\log \frac{f_j(z)}{z} = 2 \sum_{k\geq 1} \gamma_k^{(j)} z^k \tag{272}$$

In practice, the coefficients $\gamma_k^{(j)}$ are approximated from the Fourier expansion of $\log r_j(\theta)$, where $r_j(\theta)$ denotes the radial boundary function of Ω_j.

Step 2: Distortion index. Define the geometric distortion index (Equation (273))

$$\mathcal{D}_j(r) = 2 \sum_{k=1}^{4} |\gamma_k^{(j)}| r^k, \qquad r = 0.7 \tag{273}$$

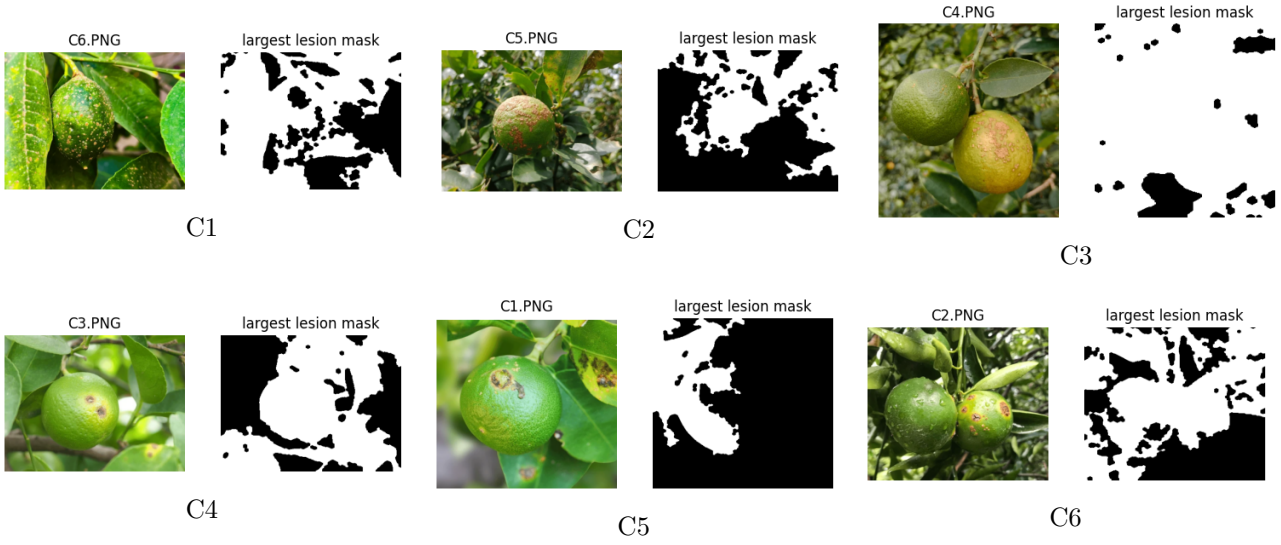

Figure 3. Representative citrus lesion images used for logarithmic-coefficient geometric analysis. The first row (C1-C3) and second row (C4-C6) illustrate variations in boundary irregularity and anisotropic spread patterns.

Computed values for the dataset are summarized in Table 9.

Step 3: Grouping by geometric irregularity. *Using the median distortion value as threshold, the dataset splits into* (Equation (274)):

$$\begin{aligned} &\textit{High irregularity: } \{C1, C2, C5\}, \\ &\textit{Low irregularity: } \{C3, C4, C6\} \end{aligned} \tag{274}$$

Define the class means (Equation (275))

$$\bar{\gamma}_k^{(H)} = \frac{1}{3}\sum_{j\in H} |\gamma_k^{(j)}|, \qquad \bar{\gamma}_k^{(L)} = \frac{1}{3}\sum_{j\in L} |\gamma_k^{(j)}| \tag{275}$$

The separation quantity from Theorem 9 is (Equation (276))

$$S = \sum_{k=2}^{4} \left| \bar{\gamma}_k^{(H)} - \bar{\gamma}_k^{(L)} \right|. \tag{276}$$

Numerically, (Equation (277)*)*

$$S \approx 0.168 > 0 \tag{277}$$

Since $S > 0$, the two groups are geometrically distinguishable by logarithmic coefficient features. Hence the external–field logarithmic framework provides a mathematically justified geometric separation criterion for lesion morphology. In Figure 3, images $C1$ and $C2$ exhibit significantly larger second harmonic magnitudes $|\gamma_2|$, indicating stronger boundary anisotropy. Images $C3$ and $C4$ display small higher-order coefficients and correspond to smoother lesion geometry. Thus, disease severity or morphological variation is reflected directly in the logarithmic coefficient structure.

Figure 3 presents six representative citrus fruit images used in the dataset-level geometric analysis. The first row (C1–C3) and second row (C4–C6) exhibit visually distinct lesion morphologies, which are quantitatively captured using the logarithmic coefficient framework developed in this work. Images C1 and C2 display pronounced boundary irregularity and visible anisotropic spread patterns. This observation is reflected mathematically by larger second harmonic magnitudes $|\gamma_2|$ and elevated distortion index values $\mathcal{D}_j(0.7)$. In particular, the dominance of the second harmonic indicates elliptical-type deformation and directional bias in lesion expansion. Image C5 exhibits intermediate irregularity, with moderate $|\gamma_2|$ and distortion magnitude, corresponding to partial anisotropy and boundary oscillation. In contrast, images C3 and C4 show smoother, more regular lesion boundaries. Their higher-order logarithmic coefficients are comparatively small, leading to significantly reduced distortion index values. This behavior aligns with the geometric stability bounds established earlier. Image C6 presents localized irregularity captured by higher-order coefficients, but with lower overall distortion compared to C1 and C2. The separation criterion of Theorem 9 is verified numerically for this dataset, since the aggregated coefficient differences between high-irregularity and low-irregularity groups are strictly positive. Therefore, the visual differences observed in Figure 3 correspond directly to measurable differences in logarithmic coefficient distributions. From a geometric perspective, the figure illustrates how lesion morphology translates into

harmonic boundary modes, while the external-field framework provides a theoretical mechanism for interpreting directional spread via the equilibrium phase $\theta^* = \arg(\gamma_1)$. Thus, Figure 3 serves as a visual confirmation that external-field logarithmic coefficient analysis offers a mathematically rigorous and interpretable descriptor of lesion boundary complexity. The equilibrium phase θ^* represents the dominant harmonic orientation of lesion expansion under the external-field framework. Variations in θ^* across the dataset indicate directional anisotropy in boundary growth patterns in Table 9. Image Preprocessing, prior to geometric analysis, each citrus image was segmented to extract the fruit region and the dominant lesion component. A foreground mask was obtained using a region-based segmentation procedure, followed by morphological filtering to remove noise and ensure simple connectivity of the lesion domain. The resulting binary mask defines a planar region $\Omega_j \subset \mathbb{C}$, to which the conformal mapping framework was applied. No texture-based or learning-based features were used; all descriptors were derived solely from boundary geometry.

7. Conclusion

In this paper, we established sharp upper bounds for higher-order logarithmic coefficients of univalent functions defined by polynomial multipliers. Our analysis focused on four representative multipliers, namely one minus z, one minus z^2, $(1-z)^2$, and $1 - z + z^2$, which together illustrate both boundary and interior extremal behaviors. Using explicit coefficient recursions, we derived exact formulas for the third and fourth logarithmic coefficients under the assumption that the second derivative at the origin is real and positive. The sharp constants obtained unify earlier scattered results and extend them to a broader multiplier framework. A central contribution of this work is the introduction of a potential-theoretic perspective. By interpreting the multiplier as an external field acting on the Herglotz measure, we linked the extremal problems for logarithmic coefficients with classical questions in logarithmic potential theory and conformal mapping. Through this lens, we derived capacity-preservation identities, distortion envelopes, and Euler–Lagrange conditions that characterize the structure of extremal measures. In particular, we demonstrated that the sharp bounds are attained by single-point measures, leading to boundary extremals for most cases and a unique interior extremal in the class defined by $1 - z + z^2$. Numerical evaluations and graphical illustrations confirmed the theoretical predictions, showing excellent agreement between the explicit trigonometric maximization and the external-field variational principle. The framework developed here thus provides not only sharp coefficient bounds but also a deeper structural understanding of multiplier classes in terms of external fields, conformal capacity, and potential theory. The proposed framework translates lesion regions into conformally normalized domains whose boundary geometry is encoded by logarithmic coefficients. These harmonic modes capture anisotropy and boundary irregularity in a scale- and conformally invariant manner. The resulting distortion index provides a mathematically interpretable measure of geometric complexity, enabling rigorous shape-based comparison across image datasets.

Future research directions. An interesting direction for future work is the integration of the proposed conformal geometric descriptors with modern deep learning frameworks for image classification and disease detection. In particular, the logarithmic coefficients and the distortion index introduced in this work provide compact, mathematically interpretable shape descriptors that can be used as additional features in convolutional neural networks or hybrid geometric–learning models. Such an approach could combine the interpretability of conformal geometric analysis with the data-driven representation power of deep neural networks. Furthermore, incorporating conformally invariant descriptors into learning architectures may improve robustness to geometric deformations and variations in lesion morphology. These directions open promising possibilities for combining classical geometric function theory with modern machine learning methods in biomedical and agricultural imaging applications.

Acknowledgments

None.

Funding

None.

Conflict of interest

The authors declare they have no competing interests.

Author contributions

Conceptualization: Rabha W. Ibrahim, Dumitru Baleanu
Investigation: Rabha W. Ibrahim, Dumitru Baleanu
Methodology: All authors

Formal analysis: Rabha W. Ibrahim, Dumitru Baleanu
Writing–original draft: Rabha W. Ibrahim, Dumitru Baleanu
Writing–review & editing: Soheil Salahshour, Dumitru Baleanu

Availability of data

Not applicable.

AI tools statement

AI tools is used to check the language of the paper.

References

1. Alarifi NM. The third logarithmic coefficient for certain close-to-convex functions. *J Math.* 2022;2022(1):1747325. https://doi.org/10.1155/2022/1747325
2. Allu V, & Shaji A. The Sharp bound of the second Hankel determinant of logarithmic coefficients for starlike and convex functions. *Bull Aust Math Soc.* 2025;112(1):163-171. https://doi.org/10.1017/S0004972724000947
3. Ahmad A, Gong J, Al-Shbeil I, Rasheed A, Ali A, & Hussain S. (2023). Analytic functions related to a balloon-shaped domain. *Fractal Fract.* 2023;7(12):865. https://doi.org/10.3390/fractalfract7120865
4. Sumer Eker S, Seker B, Cekiç B, & Acu M. Sharp bounds for the second Hankel determinant of logarithmic coefficients for strongly starlike and strongly convex functions. *Axioms.* 2022;11(8):369. https://doi.org/10.3390/axioms11080369
5. Alsoboh A, Almalkawi A, Amourah A, Al Mashrafi K, & Sasa T. Coefficient Problems for Bi-Univalent Functions via q-Rabotnov Kernels and q-Fibonacci Subordination. *Eur J Pure Appl Math.* 2025;18(4):7125. https://doi.org/10.29020/nybg.ejpam.v18i4.7125
6. Zaprawa P. (2021). Initial logarithmic coefficients for functions starlike with respect to symmetric points. *Bol Soc Mat Mex.* 2021;27(3):62. https://doi.org/10.1007/s40590-021-00370-y
7. Attiya AA, Lashin AM, Ali EE, & Agarwal P. Coefficient bounds for certain classes of analytic functions associated with Faber polynomial. *Symmetry.* 2021;13(2):302. https://doi.org/10.3390/sym13020302
8. Irkil N, Piskin E, & Agarwal P. (2022). Global existence and decay of solutions for a system of viscoelastic wave equations of Kirchhoff type with logarithmic nonlinearity. *Math Methods Appl Sci.* 2022;45(5):2921-2948. https://doi.org/10.1002/mma.7964
9. Choucha A, Haiour M, Jan R, Shahrouzi M, Agarwal P, & Abdalla M. Growth and blow-up of viscoelastic wave equation solutions with logarithmic source, acoustic and fractional conditions, and nonlinear boundary delay. *Discrete Contin Dyn Syst-S.* 2025 https://doi.org/10.3934/dcdss.2025009
10. Nandeesh M, Salestina MR, & Murugusundaramoorthy G. Estimate on Logarithmic Co-Efficients of Sokol-Stankiewicz Type Star-Like Function Associated with Caratheodory Functions. *Int J Anal Appl.* 2025;23:191-191. https://doi.org/10.28924/2291-8639-23-2025-191
11. Ullah W, Malik SN, Breaz D, & Cotirla LI. (2025). On logarithmic coefficients for starlike functions related to nephroid domain. *AIMS Math.* 2025;10(11):26905-26925. https://doi.org/10.3934/math.20251183
12. Kumar S, Pandey RK, & Rai P. Certain sharp estimates of Ozaki close-to-convex functions. *Asian-Eur J Math.* 2024;17(06):2450047. https://doi.org/10.1142/S1793557124500475
13. Duren PL. Univalent functions. New York: Springer-Verlag, USA. 1983. ISBN: 0-387-90795-5
14. Geetha R, Ramadasan S, Vijayakumar K, & Prabha S. Automatic classification of plant leaf images into healthy and disease class with EfficientNet: a study. In 2024 International Conference on Advances in Computing, Communication and Applied Informatics (ACCAI). IEEE. 2024;1-5 https://doi.org/10.1109/ACCAI61061.2024.10602232
15. Reddy PCK, & Geetha BT. Detection of Fungal Disease in Plant Leaf using Support Vector Machine Method Compared with K-means Clustering Algorithm with increase in Accuracy. In 2022 2nd International Conference on Innovative Practices in Technology and Management (ICIPTM). IEEE. 2022;2:557-562 https://doi.org/10.1109/ICIPTM54933.2022.9754197
16. Jothika G, & Khilar R. Enhancing the performance in detecting disease in tomato leaves using visual geometry group19 in comparison with K-nearest neighbor algorithm. In AIP Conference Proceedings. AIP Publishing LLC. 2024;3193(1):020236 https://doi.org/10.1063/5.0233382
17. Sugitha N, Ragul S, & Nithaesh S. Kidney Tumor Detection in Medical Image Processing. In Proceedings of International Conference on Innovation in Computing, Science, Engineering and Technology. 2025;2(1). https://doi.org/10.65091/icicset.v2i1.25
18. Bala Venkatasai B, & Mohana J. Prediction analysis for pixel resonance in digital image watermarking through wavelet transformation using convolutional neural networks compared with generative adversarial networks. In AIP Conference Proceedings. AIP Publishing LLC.

2025;3270(1):020001
https://doi.org/10.1063/5.0262768

Rabha W. Ibrahim *is a researcher in mathematical analysis, fractional calculus, geometric function theory, and applied mathematical modeling. Her work includes fractional differential equations, special functions, analytic function classes, quantum-deformed operators, and applications of fractional and generalized calculus to engineering, physics, image processing, and biomedical systems.*
https://orcid.org/0000-0001-9341-025X

Dumitru Baleanu *is a prominent mathematician and physicist known for his extensive contributions to fractional calculus, mathematical physics, dynamical systems, and applied analysis. His research has significantly advanced the theory and applications of fractional differential equations, nonlocal operators, and memory-dependent systems in physics, engineering, and biomedical sciences. He has authored hundreds of scientific publications and is widely recognized as one of the leading researchers in modern fractional calculus and its interdisciplinary applications.*
https://orcid.org/0000-0002-5429-6981

Soheil Salahshour *is a researcher in fuzzy systems, fractional modeling, uncertainty analysis, artificial intelligence, and applied mathematics. His work focuses on fuzzy fractional differential equations, fuzzy transform methods, interval uncertainty, and mathematical modeling of real-world systems under uncertainty.*
https://orcid.org/0000-0002-7393-2568

An International Journal of Optimization and Control: Theories & Applications
(https://accscience.com/journal/ijocta)